https://rbgeomorfologia.org.br/
ISSN 2236-5664

Revista Brasileira de Geomorfologia

v. 24, nº 4 (2023)

http://dx.doi.org/10.20502/rbg.v24i4.2416

Artigo de Pesquisa

Low-cost mapping of coastal geomorphology by remote sensing in Anjos Cove, Arraial do Cabo, Brazil

Mapeamento de baixo custo da geomorfologia costeira por sensoriamento remoto na Enseada dos Anjos, Arraial do Cabo, Brasil

Ruan Vargas [1], Julio Cesar de Faria Alvim Wasserman [2], Camila Américo dos Santos [3], Agenor Cunha da Silva [4] e Fábio Ferreira Dias [5]

[1] Universidade Federal Fluminense, Programa de Pós-graduação em Biologia Marinha e Ambientes Costeiros, Niterói, Brasil. E-mail: ruanvargas@id.uff.br
ORCID: https://orcid.org/0000-0001-8359-9239

[2] Universidade Federal Fluminense, Departamento de Análise Geoambiental, Niterói, Brasil. E-mail: julio.wasserman@gmail.com
ORCID: https://orcid.org/0000-0002-7828-5240

[3] Universidade Federal Fluminense, Programa de Pós-graduação em Biologia Marinha e Ambientes Costeiros, Niterói, Brasil. E-mail: camilaamerico@id.uff.br
ORCID: https://orcid.org/0000-0003-3286-3428

[4] Marinha do Brasil, Rio de Janeiro, Brasil. E-mail: prof_agenor@hotmail.com
ORCID: https://orcid.org/0000-0001-5010-6485

[5] Universidade Federal Fluminense, Programa de Pós-graduação em Biologia Marinha e Ambientes Costeiros e Programa de Pós-graduação em Engenharia de Biossistemas, Niterói, Brasil. E-mail: fabioferreiradias@id.uff.br
ORCID: https://orcid.org/0000-0003-2078-7405

Recebido: 22/05/2023; Aceito: 10/10/2023; Publicado: 09/12/2023

Abstract: Bathymetry is a crucial information for understanding coastal geomorphological processes. This study aims to evaluate the applicability of Satellite-Derived Bathymetry (SDB) as a low-cost alternative for coastal geomorphological mapping in Anjos Cove. Sentinel-2B images were used for generation of SDBs of coastal environments by two empirical methodologies. Depths were measured *in situ* by echo sounding for calibration and validation of the models. The models of Anjos Beach calibrated with 100% and 50% of the control points were evaluated for cost and time reduction. All SDBs of Anjos Beach presented similar geomorphological features and statistics results, with correlations of $r \cong 0.94$ both in calibration and validation. When considering half of the control points for model calibration, the total cost for the mapping is estimated to reduce by approximately 50%. A SDB of a submerged sandbar was also mapped with a correlation of $r \cong 0.98$ with depth field data. SDB can be used for a quick and low-cost assessment of the geomorphology in Anjos Cove. New SDB models can be evaluated from higher spatial resolution satellites to reduce errors.

Keywords: Satellite-Derived Bathymetry; coastal environments; beach; environmental monitoring;

Resumo: A batimetria é uma informação crucial para a compreensão dos processos geomorfológicos costeiros. Este estudo tem como objetivo avaliar a aplicabilidade da Batimetria Derivada de Satélite (BDS) como uma alternativa de baixo custo para o mapeamento geomorfológico costeiro na Enseada dos Anjos. Imagens Sentinel-2B foram usadas para geração de BDSs de ambientes costeiros por duas metodologias empíricas. As profundidades foram medidas *in situ* por ecossondagem para calibração e validação dos modelos. Os modelos da Praia dos Anjos calibrados com 100% e 50% dos pontos de controle foram avaliados quanto à redução de custo e tempo. Todos os BDSs da Praia dos Anjos apresentaram feições geomorfológicas e resultados estatísticos semelhantes, com correlações de $r \cong 0{,}94$ tanto na calibração quanto na validação. Considerando metade

dos pontos de controle para calibração do modelo, estima-se que o custo total do mapeamento seja reduzido em aproximadamente 50%. Um BDS de um banco de areia submerso também foi mapeado com uma correlação de $r \cong 0{,}98$ com dados de profundidade de campo. O BDS pode ser usado para uma avaliação rápida e de baixo custo da geomorfologia na Enseada dos Anjos. Novos modelos de BDS podem ser avaliados a partir de satélites de maior resolução espacial para reduzir erros.

Palavras-chave: Batimetria derivada de satélite; ambientes costeiros; praia; monitoramento ambiental.

1. Introduction

Bathymetry data have broad applications and it is a crucial information for understanding geomorphological phenomena such as coastal erosion and deposition processes on sandy beaches (e.g. KIM; LEE; MIN, 2017); monitoring of nearshore topography (e.g. MATSUBA; SATO, 2018; ALEVIZOS; ROUSSOS; ALEXAKIS, 2022); improving nautical charts (e.g. CHÉNIER; FAUCHERR; AHOLA, 2018); benthic habitat mapping (e.g. CONTI; MOTA; BARCELLOS, 2020); for coastal engineering operations such as beach nourishment (e.g. LUDKA et al., 2019; BITAN; ZVIELY, 2020), and dredging in port areas (e.g. EL-HATTAB, 2014; MATEO-PÉREZ et al., 2021). Naturally, the methods, techniques and equipment for bathymetric mapping have evolved and become more accurate over the last centuries (MENANDRO; BASTOS, 2020), as well as the first studies about bathymetry by satellite multispectral images started in 1960s and 1970s, regarded as Satellite-Derived Bathymetry (SDB), and currently by Unmanned Aerial Vehicle (UAV) (e.g. POLCYN; ROLLIN, 1969; LYZENGA, 1978; DIERSSEN; THEBERGE JR., 2014; SAYLAM et al., 2018; ROSSI; MAMMI; PELLICCIA et al., 2020).

In the 21st century, the SDB methods have become widely applied worldwide in different coastal environments and the satellites and its sensors have been extensively evaluated (applications of different spectral bands, comparison of methodologies and results obtained by different satellites), such as the Landsat series, IKONOS, Worldview family and the European Sentinel-2 (e.g. CASAL et al., 2019; EVAGOROU et al., 2019; CABALLERO; STUMPF, 2019). According to Ashphaq, Srivastava and Mitra (2021), imaging passive remote sensing methods for bathymetry mapping are accurate and relatively simple to implement. As demonstrated by Leder et al. (2023) through bibliometric analysis, the number of scientific publications about SDBs has increased during the last few years, mainly from 2017, highlighting a great interest by researchers in the use of this method to estimate depths.

Although there are several studies about development and performance of SDB algorithms, there is still a limitation in studies that explore SDBs on a specific geospatial application, and studies and works about coastal geomorphology can be widely benefited by SDB products (ALEVIZOS; ROUSSOS; ALEXAKIS, 2022). However, some authors have used SDB for mapping and monitoring coastal geomorphology, as the works by Caballero and Stumpf (2020), in which they mapped and quantified bathymetric changes (erosion/accretion) in a tidal inlet environment in the USA; by Misra and Ramakrishnan (2020), where they evaluated the geomorphological impact of a beach nourishment project using multitemporal SDB products in India; and by Alevizos, Roussos and Alexakis (2022), in which the authors mapped the evolution of submerged coastal features by high resolution satellite imagery of Worldview-3 and Geoeye-1 in Crete.

Among coastal environments, the beaches can be highlighted for their multiple uses and ecosystem services (e.g. industry, ports operations, navigation, recreation, tourism, natural coastal protection against storms, habitat for animal and plant species, etc.), nevertheless, many sandy baches worldwide are under the process of coastal erosion (LUIJENDIJK et al., 2018; VOUSDOUKAS et al., 2020) and it can be a problem for anthropic activities located in this environment. In the face of such problem, in Europe, the report "Living with coastal erosion in Europe: sediments and space for sustainability" from 2006 by EUROSION mapped the degree of exposure to coastal erosion in several European countries. In Brazil, the publication "Panorama of Coastal Erosion in Brazil" by the Ministry of the Environment – MMA (MUEHE, 2018) depicts several points of erosion along the entire Brazilian coast.

This phenomenon is related to the sedimentary balance of the coastal environment. When there is a negative sediment balance, erosion occurs and, when there is a positive balance, accretion occurs, and it is linked to the different sources of input and output of sediments in the beach system, described by Souza et al. (2005) and Bird (2008). Coastal erosion is caused by natural and/or anthropogenic factors influencing in the sedimentary balance, depending on the environmental characteristics of the coastal plain (LEATHERMAN et al., 2000; SOUZA et al.,

2005; BIRD, 2008; LUIJENDIJK et al., 2018). Also, it is directly linked to sea level rise (LEATHERMAN et al., 2000; LEATHERMAN et al., 2003) and it may be aggravated in the coming decades due to climate changes, which it is predicted a mean increase of 0.77 m (medium confidence) in Global Mean Sea Level in 2100 in the more pessimist scenario by Intergovernmental Panel on Climate Change (Sixth Assessment Report – AR6), as well as the increase in the frequency of storms (ZHANG et al., 2004; FOX-KEMPER et al., 2021).

Thus, considering the phenomenon of coastal erosion and sea level rise, bathymetry is inserted in this context as a variable intrinsically related to coastal morphodynamics. As an example, the "Bruun's rule" (Bruun, 1962), originally, is a practical form that considers the depth of closure of a beach and sea level rise to quantify the retrogradation of the coastline (erosion). Although criticized by some authors (e.g. COOPER, PILKEY; 2004) for being a generic simple two-dimensional geometric model, it is massively used in research related to coastal sediment dynamics (e.g. COZANNET, et al., 2016; ATKINSON et al., 2018; WINCKLER et al., 2023). Another example is shown by Filho et al. (2020) in a short-term condition, where the authors used depth measurements (bathymetry) of the surf zone to elaborate topographic profiles and evaluate the impacts and morphological changes (sedimentary volume) of the oceanic beaches in the state of Rio de Janeiro caused by the passage of a tropical cyclone.

Regarding anthropic interference in coastal environments, port infrastructures are commonly associated to hard structures as breakwaters and jetties that can also change the coastal morphodynamics of an adjacent beach, potentialize coastal erosion and depositions processes and even cause economic losses for tourism sector, once these structures modify the shape and wave energy that break on the beach (SAENGSUPAVANICH et al., 2008; KUDALE, 2010; NOUJAS et al. 2014; VILLENA et al. 2015; RATNAYAKE et al., 2018).

So, the implementation of a port environmental monitoring program, considering the potential physical impacts on the coastline, can be requested by the competent authorities and be decisive for the continuity of port operations. As stated by Puig et al. (2015), environmental management in the port context is increasingly necessary and practiced so that operations and business plans are in fact sustainable and compatible with legislation.

In Brazil, the ports need to be in accordance with environmental laws, such as the National Environment Policy nº 6.938/1981 that institute the Environmental Licensing, and also the National Council for the Environment (CONAMA) n° 1/86 and n° 237/97 standards, which ports must just operate if they have a valid Operating License (LO) (KITZMANN; ASMUS, KOEHLER, 2014; LIMA, 2020). Thus, the execution of Basic Environmental Programs (PBAs) of different objectives (e.g. monitoring of water quality, aquatic biota, solid waste, sedimentary dynamics, beach profile, coastline, erosion processes, etc.) can be determined as a legal requirement by competent public environmental authorities such as the Brazilian Institute for the Environment and Renewable Natural Resources (IBAMA).

On this basis, SDB is regarded as a practical complementary method to the more traditional ones for measuring depths, with wide coverage of the Earth's surface by the satellite sensor, providing a fast and repetitive mapping, although they do not have the very high accuracy provided by Airborne Lidar Bathymetry (ALB) and echo sounding systems (CAHALANE et al., 2019; CABALLERO, STUMPF, 2019; CASAL et al., 2019). Thus, this study aims to evaluate the applicability of SDBs for coastal geomorphological mapping as a low-cost alternative by comparing two existing empirical methodologies.

2. Study area

The study area is located in Anjos Cove in the municipality of Arraial do Cabo, state of Rio de Janeiro, southeastern Brazil, where the Forno Port facilities are situated (Figure 1). In addition, a marina for fishermen and tourism activities are present. The Anjos Beach is a relatively small sandy beach located between two rocky headlands characterized by the predominance of fine sand and an extension of approximately 1,200 m (VILLENA et al., 2015; MOTTA et al., 2018; COLAÇO et al., 2021). In this region, the coast is characterized by changing its orientation from Northeast-Southwest to East-West, due to the fracture zone of Rio de Janeiro (MUEHE, 1998; MOTTA et al., 2018; COLAÇO et al., 2021) and is the frontier zone between the sedimentary basins of Santos and Campos (MOTTA et al., 2018).

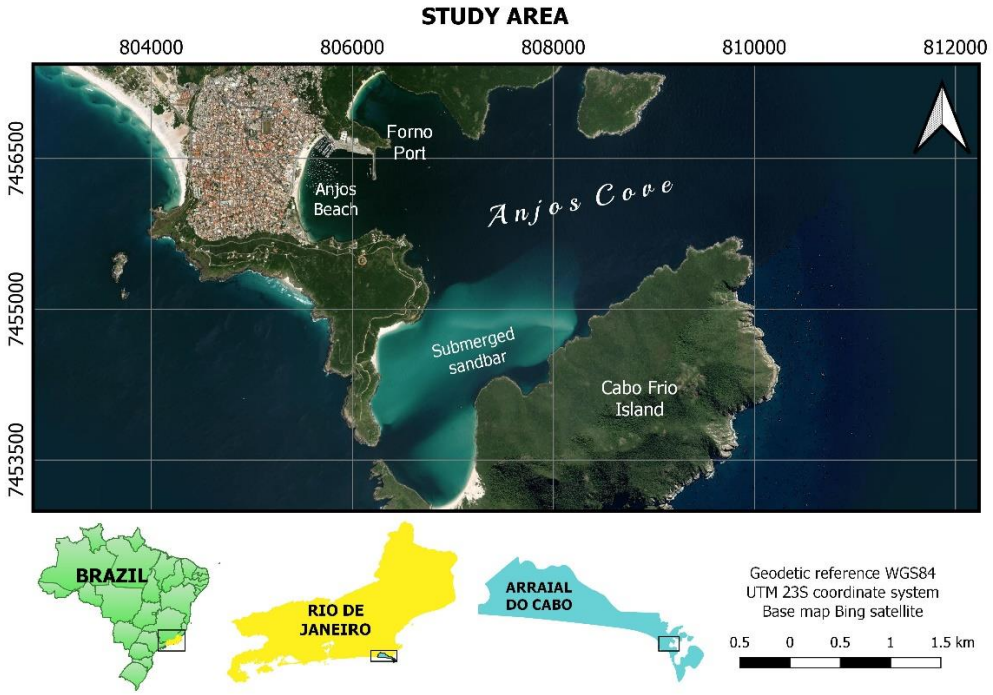

Figure 1. Location of the study area. Anjos Beach, Forno Port and the indication of the submerged sandbar.

The study area comprises the continental shelf of the Campos Basin (Bacia de Campos) geological micro compartment, between the 10 and 150 m isobaths, in which its origin and formation are associated with the rifting of the paleocontinent Gondwana (Brazil-Africa) approximately 130 million years ago (MUEHE, 1998; FIGUEIREDO JR et al., 2015). Also, the continental shelf covering the study area is characterized as a smoothed platform with a predominance of lithoclastic terrigenous sandy sediments related to the Quaternary sea level oscillation events (FIGUEIREDO JR et al., 2015).

The origin and formation of the coastal plain and features of Arraial do Cabo are related to regressive and transgressive sea level events during the Quaternary period (DIAS, CASTRO, SEOANE, 2014; JESUS et al., 2017). Jesus et al. (2017) constructed a holocenic curve of relative sea level for the region, based on altimetric measurements and radiometric dating of biological indicators of sea level (subfossils of gastropod vermetids) found in Armação dos Búzios. The authors verified that the relative sea level was below the current one between 8,148-6,300 cal yr BP, a rising sea level episode between 6,300-4,500 cal yr BP crossing the current level and reaching a transgressive maximum of approximately 2.4m, and after a lowering from 4,500 cal yr BP to present. Specifically, for Anjos Cove, Dias, Castro and Seoane (2014) carried out a paleoenvironmental reconstruction during the Pleistocene-Holocene transition based on geological indicators of sea level (beachrocks) and concluded that the relative sea level varied by approximately 6m, being a negative variation of -4.5m and a positive variation of 1.5m. The authors found that the relative sea level was 1.5m higher between 13,130-12,860 cal yr BP and -4.5m lower than the current one between 11,940-11,240 cal yr BP.

Meteorologic conditions are characterized by winds from directions between north and east are predominant and are incident during 68% with speeds of up to 5m/s during 60% of the interval, in which the months of January and August have the highest incidence, associated with the South Atlantic Subtropical Anticyclone (SASA) (BULHÕES et al., 2014; DIAS, CASTRO, SEOANE, 2014; MOTTA et al., 2018; REBOITA et al., 2019; COLAÇO et al., 2021). Cold front episodes (low pressures systems) cross the region seasonally, generating southwest and south winds and waves, usually associated with storm surges (DIAS, CASTRO, SEOANE et al., 2014; QUADROS et al., 2016; COLAÇO et al., 2021). Oceanographic conditions are characterized by waves from the NE quadrant occur during 53.5% of the interval with a mean significant height of 1.6m and period of 9s, and waves from the SE-SW quadrants occur during 45.5% (MOTTA et al., 2018). The tide is micro tidal, semi-diurnal and asymmetrical type, reaching an amplitude of 1.0 m during spring tide (SILVA, 2009). Also, the upwelling phenomenon occurs in the region during spring and summer (FERREIRA, 1998; BARBOSA et al., 2003; MELO et al., 2009).

Forno Port has approximately a century of history (PEREIRA, 2010; MOURA, 2012) and the port was modernized and expanded during 20th century, just as the municipality of Arraial do Cabo was urbanized (SAVI, 2003a; SAVI, 2003b). However, it was only in 1955 that the construction of the first breakwater began, completed in 1959 and later expanded in 1981 (SAVI, 2003b). The breakwater has a length of approximately 250 m and closes across Anjos Beach by approximately 35% (Figure 2a) (SAVI; FERNANDEZ, 2007). This resulted in a new wave regime on the beach and, consequently, rockfills were placed on the southern region of the beach at the facilities of Almirante Paulo Moreira Sea Studies Institute (IEAPM) to contain the wave actions (Figure 2b). Thus, the beach has begun showing erosive processes indicators by distinct morphodynamical characteristics in its southern (intermediate state) and northern (reflective state) sectors due to wave diffraction caused by the breakwater, also associated with anthropic occupations within the active profile of the beach system and suppression of the coastal vegetation environment (MUEHE; LINS-DE-BARROS, 2016).

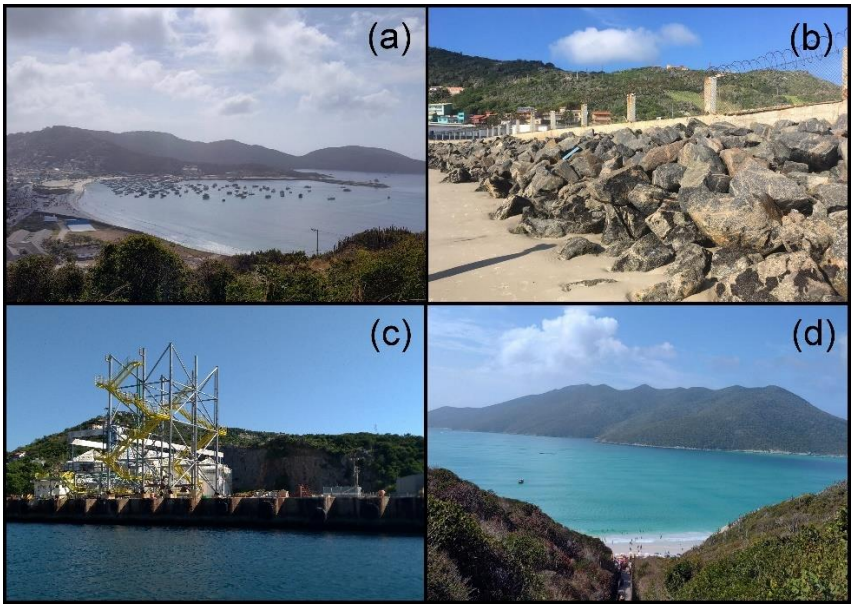

Figure 2. (a) Views of Anjos Beach. Note the large presence of boats. (b) Rockfill to contain erosion in front of IEAPM. (c) Forno Port facilities. (d) View from the continent of the submerged sandbar area and the Cabo Frio Island.

Regarding the submerged sandbar (Figure 1 and 2d), this is a depositional feature of elongated geometry located in a semi-closed cove between the mainland and Cabo Frio Island approximately 2 km from Anjos Beach. The sediments are predominantly mobilized by waves and currents from the NE quadrant (good weather) favoring their accumulation in the central part (this is well observed in Figure 1 by the presence of wave breaks), and periodically from S/SW during passages of polar cold fronts, causing erosion of the finer sediments (SILVA, 2009; CASTRO, 2018). Also, there is a tidal influence (micro tidal, semi diurnal and asymmetric) with currents acting in alternating flows in the SW-NE directions (SILVA, 2009). In this way, its geomorphology is adjusted according to the oceanographic and meteorological conditions that are acting during a period of time.

3. Materials and methods

3.1 Sentinel-2 satellite data

The Sentinel-2 mission (Sentinel-2A and B satellites) provides 13 spectral bands with spatial resolution of 10, 20 and 60 m and 12-bit of radiometric resolution. Together, they offer a temporal resolution of 5 days in the Equator region or 10 days with just one satellite (EUROPEAN SPACE AGENCY – ESA, 2015). However, only the visible and near infrared (NIR) bands (10 m of spatial resolution) were used throughout the processing.

Sentinel-2B multispectral images provided by the Multispectral Instrument (MSI) sensor in Level-2A processing were downloaded from ESA website (https://scihub.copernicus.eu/dhus/#/home), where it is freely available and were used to construct SDB models. Level-2A corresponds to Bottom-of-Atmosphere (BOA) reflectance, orthorectified in UTM coordinate system and WGS84 geodetic reference images. At this processing

level, the image is radiometric, geometric and, mainly, atmosphere corrected (ESA, 2015). Furthermore, this satellite was chosen because it is the only freely available in Brazil with the highest spatial and temporal resolutions for the purpose of this study, compared to Landsat series, since the study area is relatively small.

The scene (S2B_MSIL2A_20201002T125309_N0214_R052_T23KRQ_20201002T151006) from October 2nd, 2020 (sensing at 12:53:09.024Z) was used for the bathymetric mapping on Anjos Beach and selected for its low scene cloud coverage (0.034%) and, mainly, for the proximity of the field survey date (echo sounding). The scene (S2B_MSIL2A_20190620T125319_N0212_R052_T23KQQ_20190620T163226) from June 20th, 2019 (sensing at 12:53:19.024Z) was used for the bathymetric mapping of a submerged sandbar feature near Anjos Beach (Figure 1 and 2d). In addition, this image was chosen because the date is close to the bathymetric data collected in the field (April, 2019).

3.2 Echo sounding

Echo sounding was carried out at Anjos Beach on October 1st, 2020 for depth measurements with a single beam echo sounder, and a second campaign on November 18th, 2020 as complement, following the methodology employed by Carvalho et al. (2018) and Vargas et al. (2020), once it allows to eliminate the tide effect and normalize depths to Mean Lowest Low Water (MLLW) (local reduction level). A pair of geodetic Global Navigation Satellite System (GNSS) receivers was used for coordinates recording. One of the receivers was positioned at the SAT GPS 96327 station of the Brazilian Institute of Geography and Statistics (IBGE) (coordinates 22º58'14.94742''S and 42º01'01.48898''W), located in Forno Port. The other one was associated with the echo sounder installed on a vessel and operated in kinematic mode. Thus, each depth point recorded by the echo sounder had an associated coordinate by Differential Global Positioning System (DGPS).

The GNSS data was post-processed on GTR Processor software. This procedure generated a table containing time, latitude, longitude and ellipsoidal height (h) in the WGS84 reference system. This information was associated with depth recorded by the echo sounder through the time of tracking (hour, minute, second) by both equipment. Thus, the depths of both surveys campaign were normalized for MLLW by Eq. (1) (CARVALHO et al., 2018):

$$D_{(t)} = P_{(t)} - h_{(t)} + N + L \quad (1)$$

where *D(t)* is the corrected depth for MLLW in meters at instance *t*; *P(t)* is the observed depth in meters at instance *t*; *h(t)* is the ellipsoidal height recorded at instance *t*; N is the local geoid undulation = -5.8787 m; and L is the local difference between MSL and MLLW = -0.5197 m.

The MLLW depths were considered as "true ground points" and were randomly grouped into control points for image calibration and check points for statistical analysis and validation of SDB models, but considering the spatial and depth distribution. For image calibration, just half of the points registered on October 1st, 2020, were used, while for validation the other half of this campaign added with the points of the second campaign (November 18th, 2020) were combined.

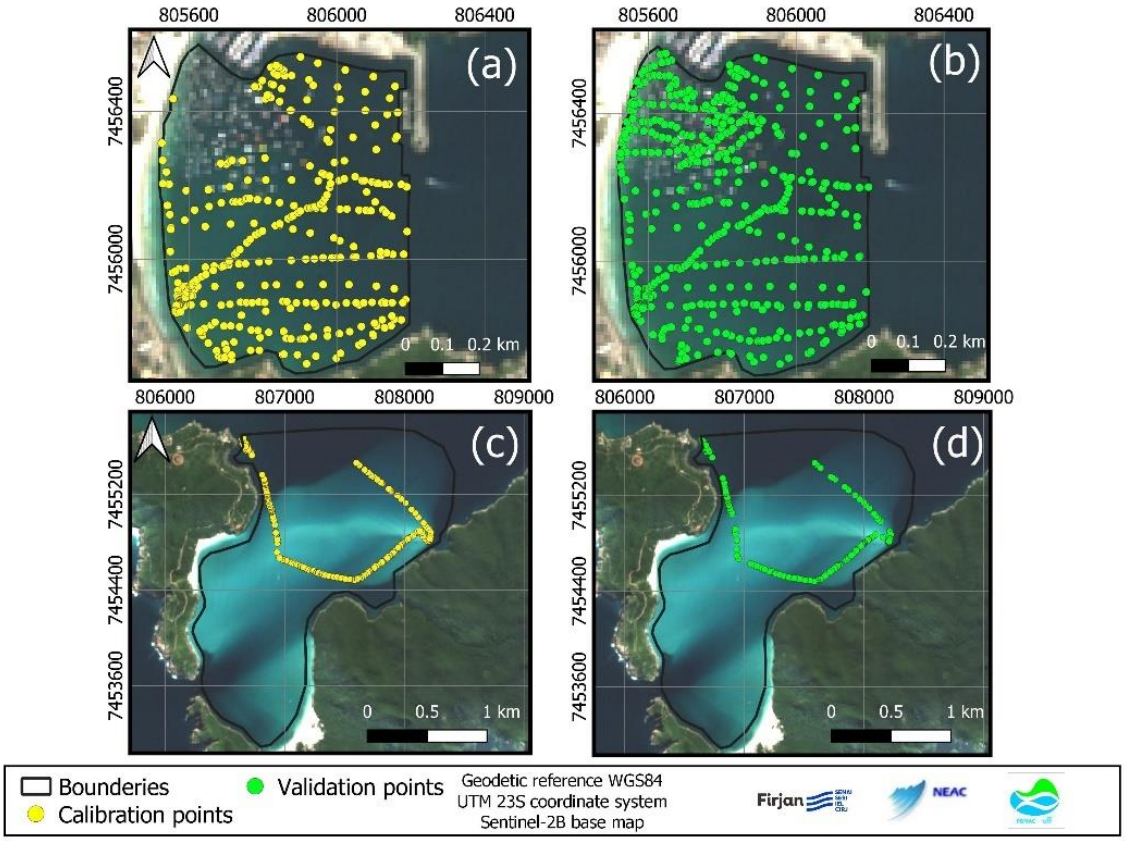

Figure 3. *In situ* depth points up to –13 m measured with the single beam echo sounding. (a) depth points used for image calibration (n = 313) and (b) depth points used for SDB validation (n = 452) on Anjos Beach. (c) depth points used for image calibration (n = 254) and (d) depth points used for SDB validation (n = 177) in the sandbar region.

Regarding the submerged sandbar bathymetric mapping, depth points were measured previously on April 4th, 2019, by single beam echo sounding following the same methodology used at Anjos Beach. However, the GNSS base was positioned at the SAT GPS 91783 station of the IBGE (coordinates 22º58'42.48583''S and 42º01'12.94081''W) located in IEAPM. The depth points were also divided between control and check points (Figure 3c and d).

3.3 Estimating depths by optical satellite images

In this study, for SDB mappings, the empirical methodologies by Lyzenga (1985) and Stumpf, Holderied and Sinclair (2003) were applied, as well as also applied by Gabr, Ahmed and Marmoush (2020), Rossi, Mammi and Pelliccia (2020) and Westley (2021). For the mapping of the submerged sandbar, just the methodology by Stumpf, Holderied and Sinclair (2003) was performed. All processing to generate SDBs was done in QGIS 3.10 and excel softwares and is represented in Figure 4.

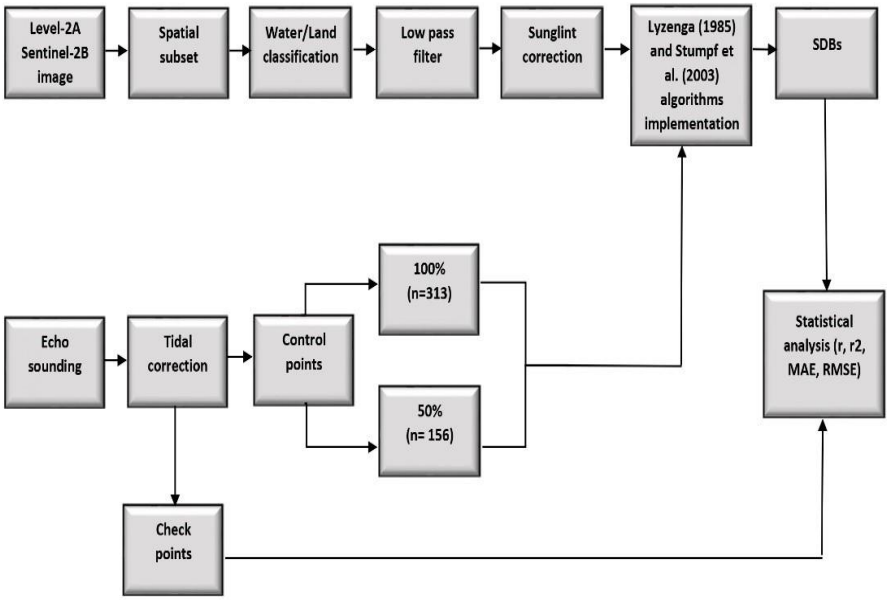

Figure 4. Methodological workflow for SDB mapping. The reduction of control points in 50% was evaluated only for the SDBs in Anjos Beach site.

These empirical methodologies are based on simple statistical relationships between *in situ* depth samples points and radiometric values of optical satellite images (pixels), preferably Bottom-of-Atmospheric (BOA) reflectance values (KUMARI; RAMESH, 2020; ASHPHAQ; SRIVASTAVA; MITRA, 2021). However, for extraction of depth information from satellite image, some pre-processing steps must be performed such as: classify water and non-water features, filter pass and sunglint correction (e.g. MISRA; RAMAKRISHNAN, 2020; VARGAS et al., 2021).

3.3.1 Classifying water and non-water features

First, the image was clipped to cover only the study area and shorten processing time. The classification of water and non-water features was performed by applying the NDWI (Normalized Difference Water Index) spectral index (MCFEETERS, 1996). This index classifies the pixels in a range of -1 to +1, where ≤ 0 values represent non-water features and > 0 represent water features. This step is essential to mask the boats on Anjos Beach and exclude them from processing. Since no boats were identified in the Sentinel-2B image from 2019 (submerged sandbar region), this step was performed only on the image from 2020. For this, Eq. (2) was applied (MCFEETERS, 1996):

$$NDWI = \frac{\rho_{(\lambda g)} - \rho_{(\lambda nir)}}{\rho_{(\lambda g)} - \rho_{(\lambda nir)}} \quad (2)$$

where $\rho_{(\lambda g)}$ is the spectral reflectance of green wavelength; and $\rho_{(\lambda nir)}$ is the spectral reflectance of the near infrared wavelength.

3.3.2 Sunglint correction

Afterwards, a 3x3 low-pass filter was applied to remove noise and the sunglint correction could be performed. This is an optical phenomenon that occurs when sunlight reflects off the surface of water at the same angle that a satellite sensor views it and interferes in the bathymetric estimation, so this must be corrected when the images present this characteristic (NATIONAL AERONAUTICS AND SPACE ADMINISTRATION – NASA, 2021). For this, the equation by Hedley, Harborne and Mumby (2005) was applied:

$$\rho`_{(\lambda i)} = \rho_{(\lambda i)} - b_{(\lambda i)}\left(\rho_{(\lambda nir)} - M_{(\lambda_{nir})}\right) \quad (3)$$

where $\rho`_{(\lambda i)}$ is the sunglint corrected pixel for wavelength i; $\rho_{(\lambda i)}$ is the reflectance of the wavelength i; $b_{(\lambda i)}$ is the regression slope; and $M_{(\lambda_{nir})}$ is the minimum value of the infrared wavelength.

2.4.3 Empirical SDBs algorithms application

The methodologies by Lyzenga (1985) and Stumpf, Holderied and Sinclair (2003) assume the water surface reflectance is an exponential function of water depth. Visible wavelengths are used to extract depth information from water bodies by remote sensing, once blue and green lights have a greater capacity to penetrate in water (deeper waters), while red light has a lower capacity (shallower waters) (STUMPF; HOLDERIED; SINCLAIR, 2003; CABALLERO; STUMPF, 2019). However, optically active constituents, the inherent optical properties (IOPs) (e.g. phytoplankton, dissolved organic matter and suspended sediments) interfere the way the electromagnetic radiation penetrates in water and modify its spectral behaviour, which can degrade the quality of bathymetric information (GAO, 2009).

For the study area (Figure 1), it was considered that the IOPs and bottom type are homogeneous. First, the Lyzenga (1985) model was applied only on Anjos Beach using blue, green and red bands:

$$Z = a_0 + \sum_i^n a_i X_i \tag{4}$$

$$Xi = Ln\left(\rho`_{(\lambda i)} - \rho`_{d(\lambda i)}\right) \tag{5}$$

where *Z* is the estimated depth; a_0 and ai are coefficients determined by multiple linear regression; and $\rho`_{d(\lambda i)}$ is the deep-water reflectance of the *i* band image with sunlight corrected. If the image is atmospherically corrected, $Xi = Ln\left(\rho`_{(\lambda i)}\right)$ (GREEN; EDWARDS; MUMBY, 2000; GABR; AHMED; MARMOUSH, 2020).

Afterwards, the Stumpf, Holderied and Sinclair (2003) model was applied on Anjos Beach and to map the submerged sandbar by Eqs. (6) and (7) (CABALLERO; STUMPF, 2020):

$$Z = m_1(pSDB) - m_0 \tag{6}$$

$$pSDB = \frac{Ln\left(n*\rho`_{(\lambda b)}\right)}{Ln\left(n*\rho`_{(\lambda g)}\right)} \tag{7}$$

where pSDB is "pseudo" bathymetry; m_1 (scale) and m_0 (offset) are constants (coefficients) determined by linear regression; *n* is a fixed constant for the entire area; $\rho`_{(\lambda b)}$ is the sunglint corrected reflectance of blue wavelength; and $\rho`_{(\lambda g)}$ is the sunglint corrected reflectance of green wavelength.

Aiming to reduce costs and time for bathymetric mapping on Anjos Beach, the sentinel-2B image of both models (Lyzenga and Stumpf) were calibrated with 100% (n=313) and 50% (n=156) of the control points for comparison. For validation, the previously separated bathymetric check points were used (Figure 3b), correlating them with their respective estimated SDBs values. Thus, the Pearson and determination coefficients, Mean Absolute Error (MAE) and Root Mean Square Error (RMSE) were calculated, following the studies by Mateo-Pérez et al. (2020) and Vargas et al. (2021).

3. Results

3.1 Anjos Beach SDB mapping

3.1.2 Lyzenga bathymetry models

Regarding the bathymetric models generated by Lyzenga (1985) methodology, Table 1 presents the statistical results of the image calibration step by multiple linear regression:

Table 1. Statistical parameters of image calibration by Lyzenga methodology in the depth range of 0-12 m on Anjos Beach considering 100% (n = 313) and 50% (n = 156) of the control points.

Image x Depth points (control)	Coefficients (n = 100%)	Coefficients (n = 50%)	P-Value	*r* (n = 100%)	Adjusted r^2 (n = 100%)	*r* (n = 50%)	Adjusted r^2 (n = 50%)	Significance F
Intersection	18.0244	25.4199	P < 0.05					
Blue	25.7877	23.9073	P < 0.05	0.94	0.87	0.94	0.88	0.00
Green	-28.9129	-29.2573	P < 0.05					
Red	1.4800	2.6896	P < 0.05					

The equations for bathymetric models considering 100% and 50% of the control points were respectively:

$$Z_{(100\%)} = 18.0244 + \left[25.7877 * Ln\left(\rho`_{(\lambda b)}\right)\right] + \left[-28.9129 * Ln\left(\rho`_{(\lambda g)}\right)\right] + \left[1.4800 * Ln\left(\rho`_{(\lambda r)}\right)\right] \quad (8)$$

$$Z_{(50\%)} = 25.4199 + \left[33.9073 * Ln\left(\rho`_{(\lambda b)}\right)\right] + \left[-29.2573 * Ln\left(\rho`_{(\lambda g)}\right)\right] + 2.6896 * Ln\left(\rho`_{(\lambda r)}\right)\right] \quad (9)$$

where $Z_{(100\%)}$ is the estimated depth considering 100% of the control points; $Z_{(50\%)}$ is the estimated depth considering 50% of the control points; $\varrho`_{(\lambda b)}$ is the sunglint corrected reflectance of blue wavelength; $\varrho`_{(\lambda g)}$ is the sunglint corrected reflectance of green wavelength; and $\varrho`_{(\lambda r)}$ is the sunglint corrected reflectance of red wavelength.

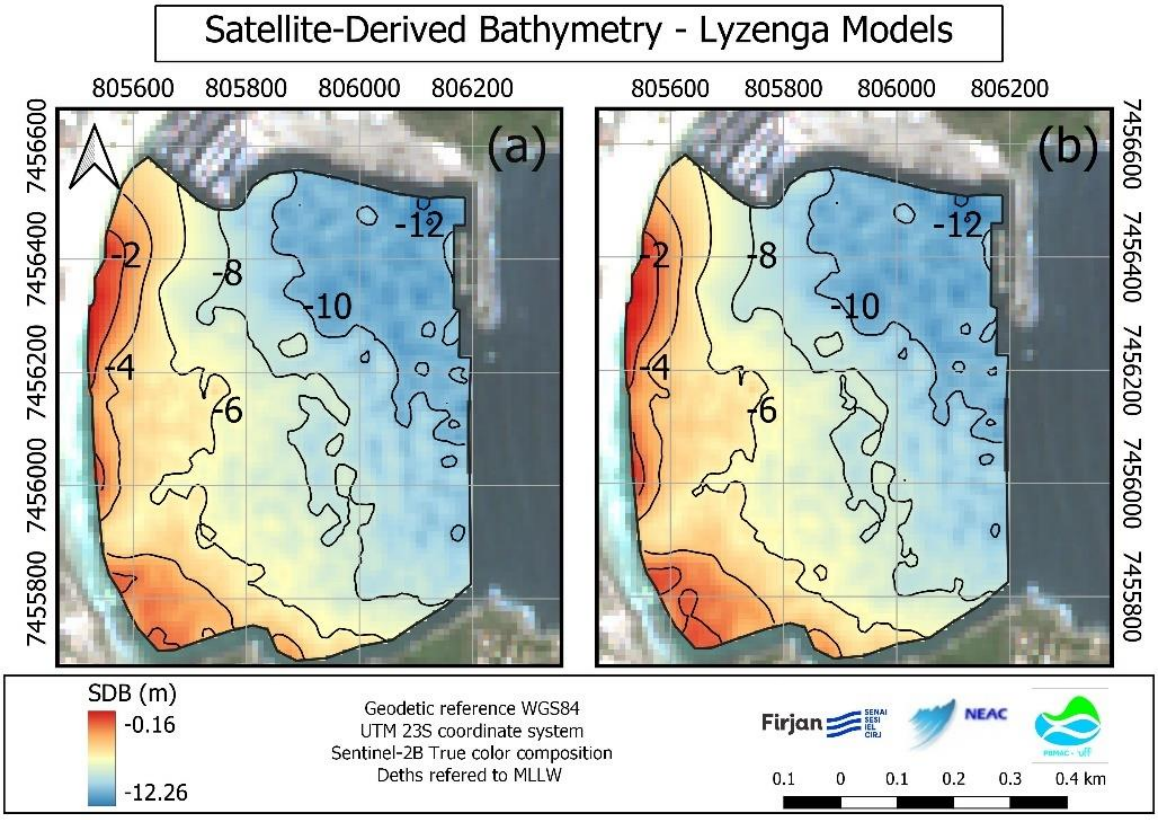

Figure 5. SDBs on Anjos Beach by Lyzenga method. (a) SDB calibrated with 100% of the calibration points (n = 313). (b) SDB calibrated with = 50% of the calibration points (n = 156).

It can be seen, through the bathymetric maps in Figure 5, both models were spatially and geomorphologically similar by comparing the isobaths. Therefore, by the representation of the isobaths, there were practically no changes in the submerged geomorphology considering the models calibrated with 100% or 50% of the control points.

Both models (Figure 5a and b) were able to represent shallower regions closer to the shoreline and deeper regions as it approaches the Forno Port and moves away from the shoreline. The -10 and -12 m isobaths evidence the deeper region, where vessels are moored. However, the SDBs were statistically evaluated by the previously separate checkpoints (Figure 3).

Table 2. Statistical parameters of bathymetric models validation by Lyzenga methodology considering 0-12 m depth range on Anjos Beach.

SDB (Lyzenga) x Depth points (Check)	*r*	r^2	P-value for *r*	MAE (meters)	RMSE (meters)	*n* (check points)
SDB A (calibrated with 100% of control points)	0.94	0.87	P < 0.01	0.78	0.97	452
SDB B (calibrated with 50% of control points)	0.93	0.86	P < 0.01	0.823	1.03	

3.1.3 Stumpf bathymetry models

Regarding the bathymetric models generated by Stumpf, Holderied and Sinclair (2003) methodology on Anjos Beach, Figure 6 illustrates the correlation results of the calibration step by linear regression:

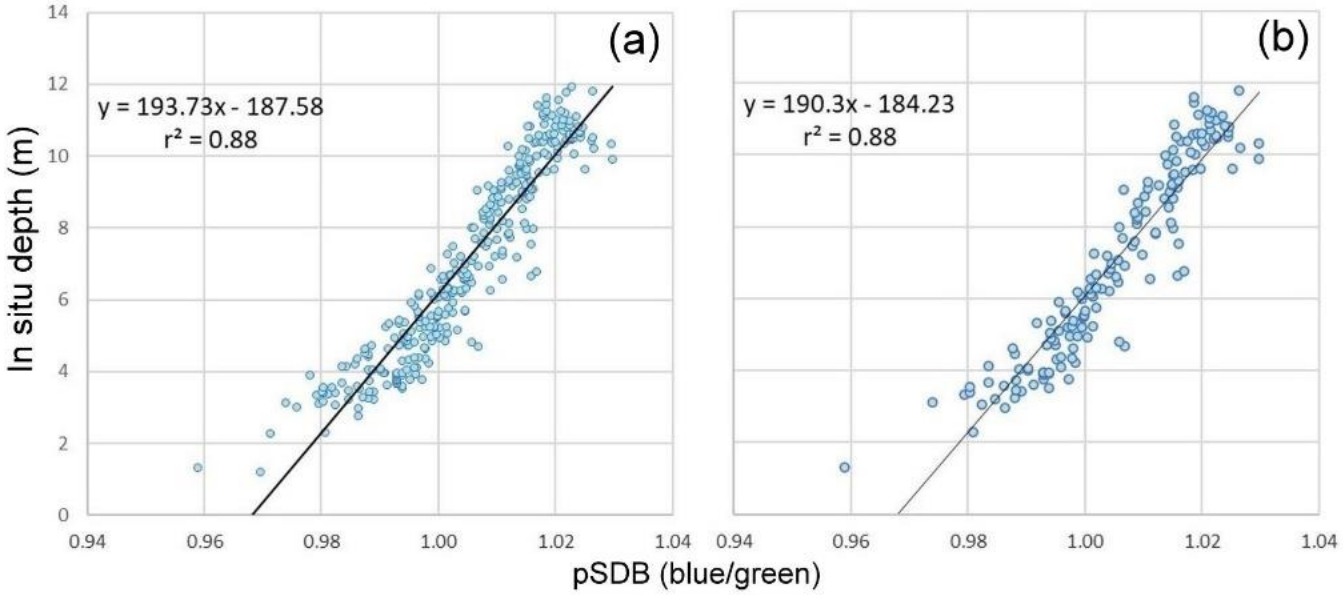

Figure 6. Scatter plot of pSDB versus *in situ* depth points on Anjos Beach. (a) Image calibration considering 100% of control points (n = 313). (b) Image calibration considering 50% of control points (n = 156).

Table 3. Statistical parameters of image calibration by Stumpf, Holderied and Sinclair (2003) methodology in the 0-12 m depth range on Anjos Beach considering 100% (n = 313) and 50% (n = 156) of the control points.

pSDB x Depth points (control)	*r*	r^2	P-value for *r*	m_1 (Coefficient)	m_0 (Coefficient)	Significance F	*n*
0-12 m	0.94	0.88	P < 0.01	193.73	187.58	0.00	313
	0.94	0.88	P < 0.01	190.3	184.23	0.00	156

After linear regression and coefficients calculation, the bathymetric maps were elaborated by Eqs. (6) and (7) and illustrated in Figure 7:

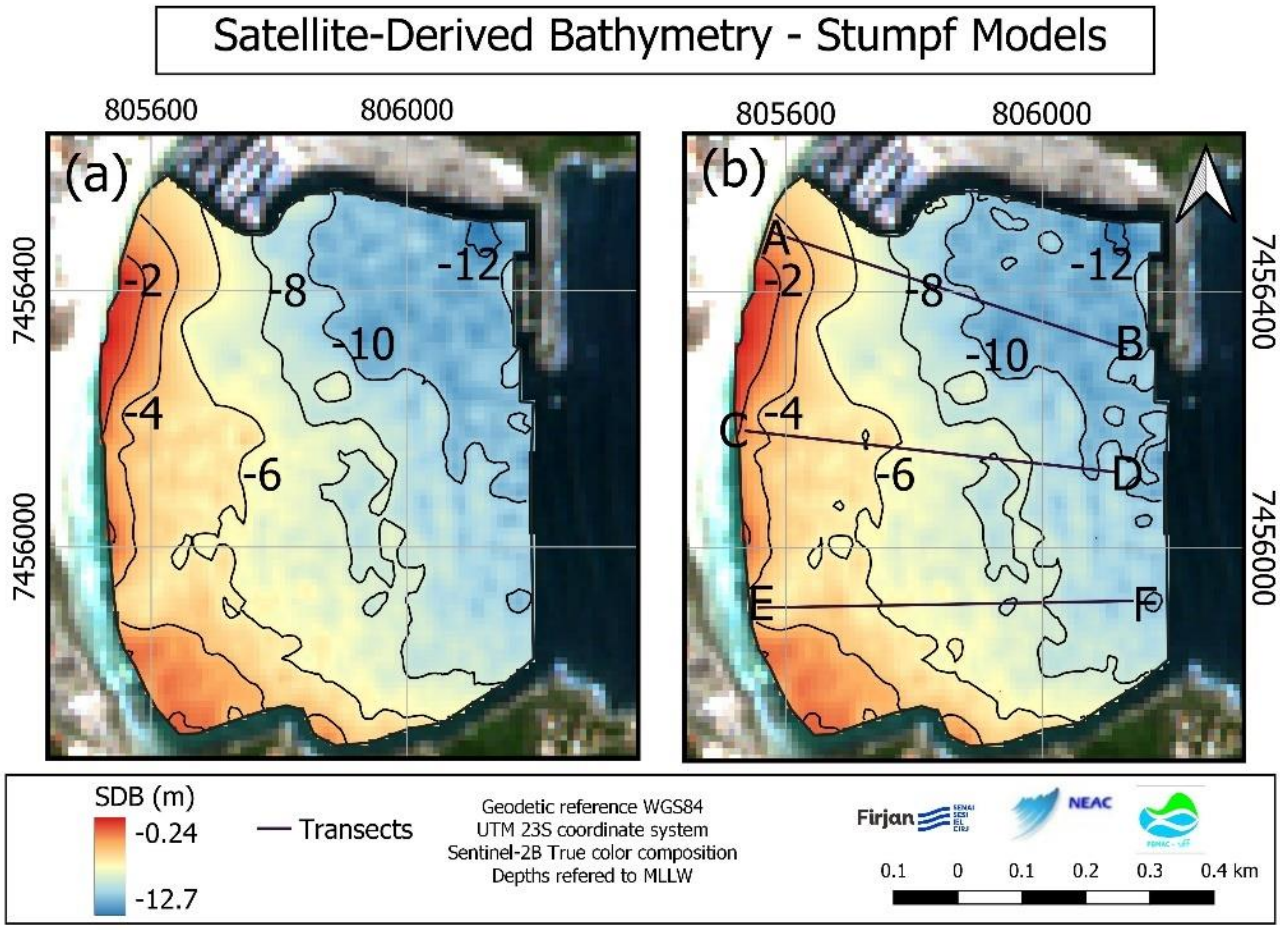

Figure 7. SDBs of Anjos Beach utilizing Stumpf method. (a) SDB calibrated with 100% of the control depth points (n=313). (b) SDB calibrated with 50% of the control depth points (n=156). Lines A-B, C-D and E-F are cross-shore transects for bathymetric profiles extraction.

The SDB models generated by the Stumpf, Holderied and Sinclair (2003) methodology, calibrated with 100% and 50% of the control points, also showed similar geomorphological (isobaths) and spatial characteristics, in which they were able to represent shallower regions near the shoreline and deeper regions near Forno Port, similarly to the models generated by Lyzenga (1985) methodology.

Table 4. Statistical parameters for validation of bathymetric models by Stumpf methodology considering 0-12 m depth range on Anjos Beach.

SDB (Stumpf) x Depth points (Check)	*r*	r^2	P-value for *r*	MAE (meters)	RMSE (meters)	n (check points)
Model A (SDB calibrated with 100% of control points)	0.94	0.88	P < 0.01	0.74	0.91	452
Model B (SDB calibrated with 50% of control points)	0.94	0.88	P < 0.01	0.74	0.91	

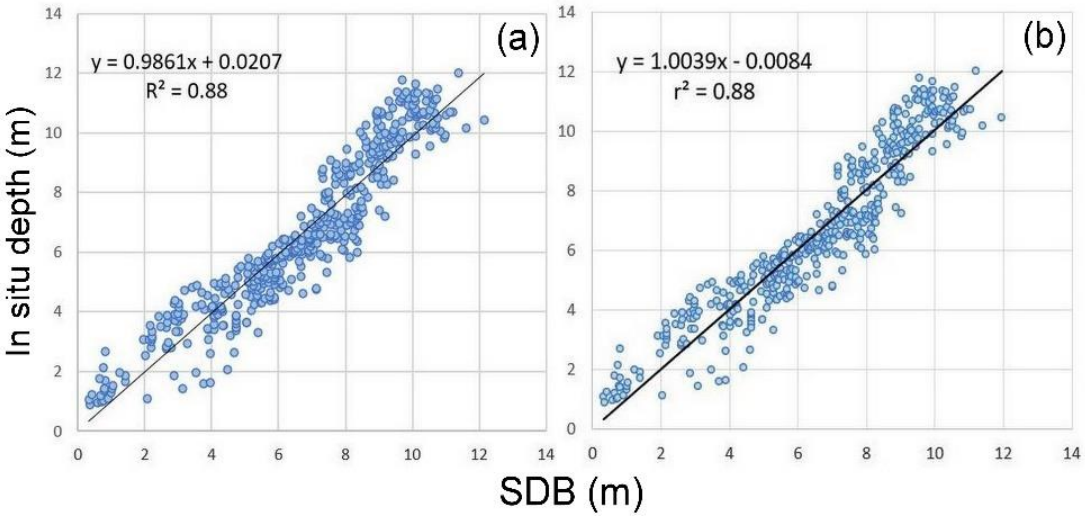

Figure 8. Scatter plot of SDBs versus *in situ* depth points on Anjos Beach. (a) SDB calibrated with 100% of control points. (b) SDB calibrated with 50% of control points. Check points (n = 452).

Comparing Tables 2 and Table 4, *r* and r^2 values for all models were correlated, especially when comparing the models calibrated with 100% and 50% of the control points, in which all of them resulted in $r \cong 0.94$ both in calibration and validation steps. These results indicate that the two empirical algorithms applied generated similar results.

Bathymetric profiles (transects A, B and C – Figure 7b) were extracted from the SDB calibrated with 50% of the control points and compared with the bathymetry made by echo sounding (ground truth). Also, the SDB performed in 2019 presented by Vargas et al. (2021) was compared with echo sounding points and with the SDB from 2020, based on the representation of isobaths and cutfill analysis.

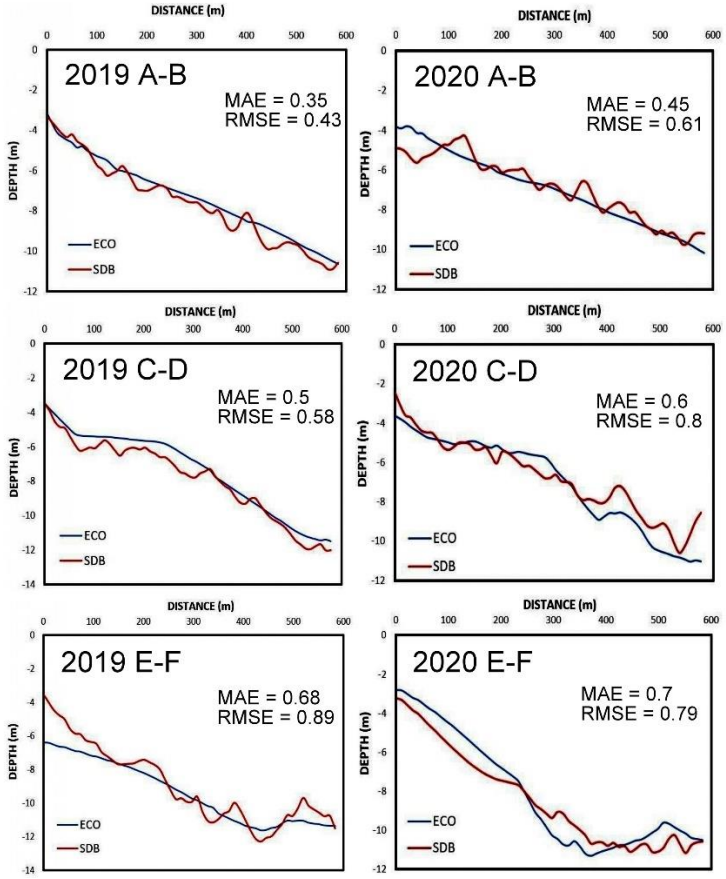

Figure 9. Bathymetric profiles of transects A-B, C-D and E-F extracted from the SDB of Anjos Beach calibrated with 50% of control points and compared with echo sounding data. Bathymetry from 2019 provided by Vargas et al. (2021) (left column) and bathymetry from 2020 elaborated in this study (right column).

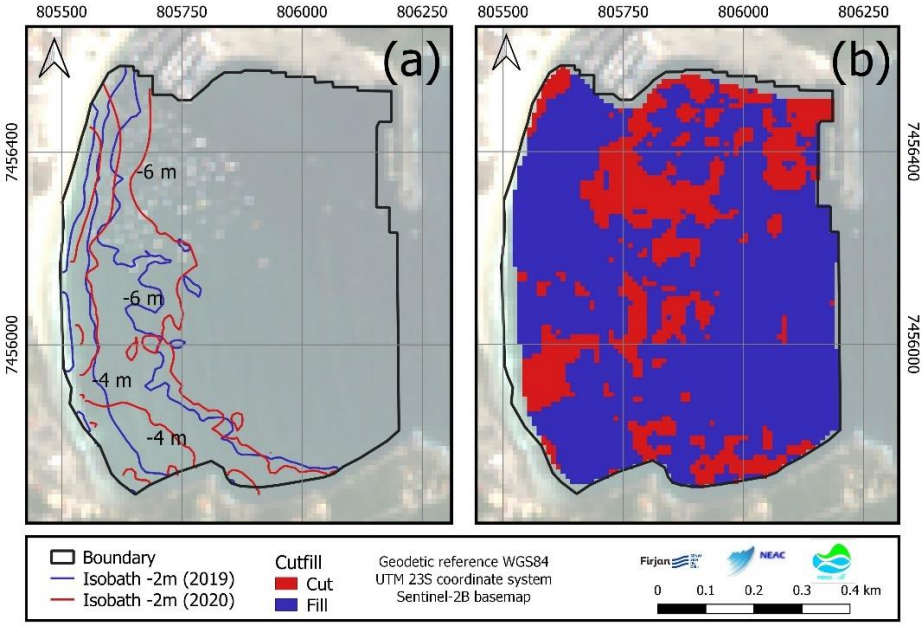

Figure 10. (a) Comparison of the isobaths extracted from 2019 and 2020 SDBs. (b) cutfill between the 2019 and 2020 SDBs.

3.2 Submerged sandbar mapping

Regarding the sandbar bathymetric mapping, Figure 11 illustrates the correlation results of the image calibration step by linear regression:

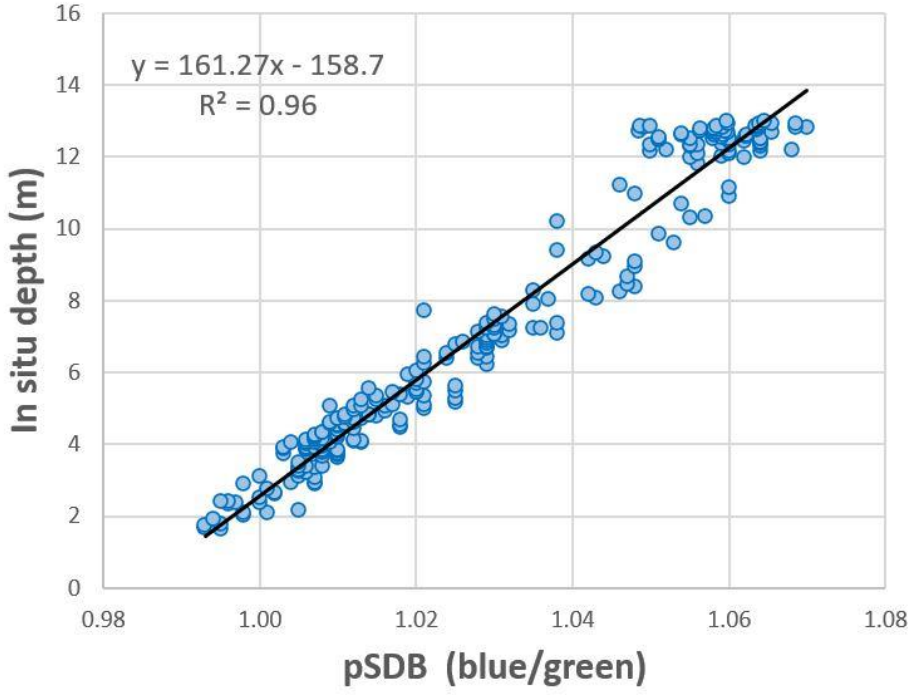

Figure 11. Scatter plot of pSDB versus *in situ* depth points on sandbar region (n = 254).

Table 6. Statistical parameters of image calibration by Stumpf, Holderied and Sinclair (2003) methodology in the 0-12 m depth range in the submerged sandbar region.

Statistics	***r***	***r*²**	**P-value for *r***	**n (calibration points)**
pSDB (Stumpf) x Depth points (calibration)	0.98	0.96	P < 0.01	254

Applying the equation generated in the calibration step (Figure 11), the SDB of the submerged sandbar was generated:

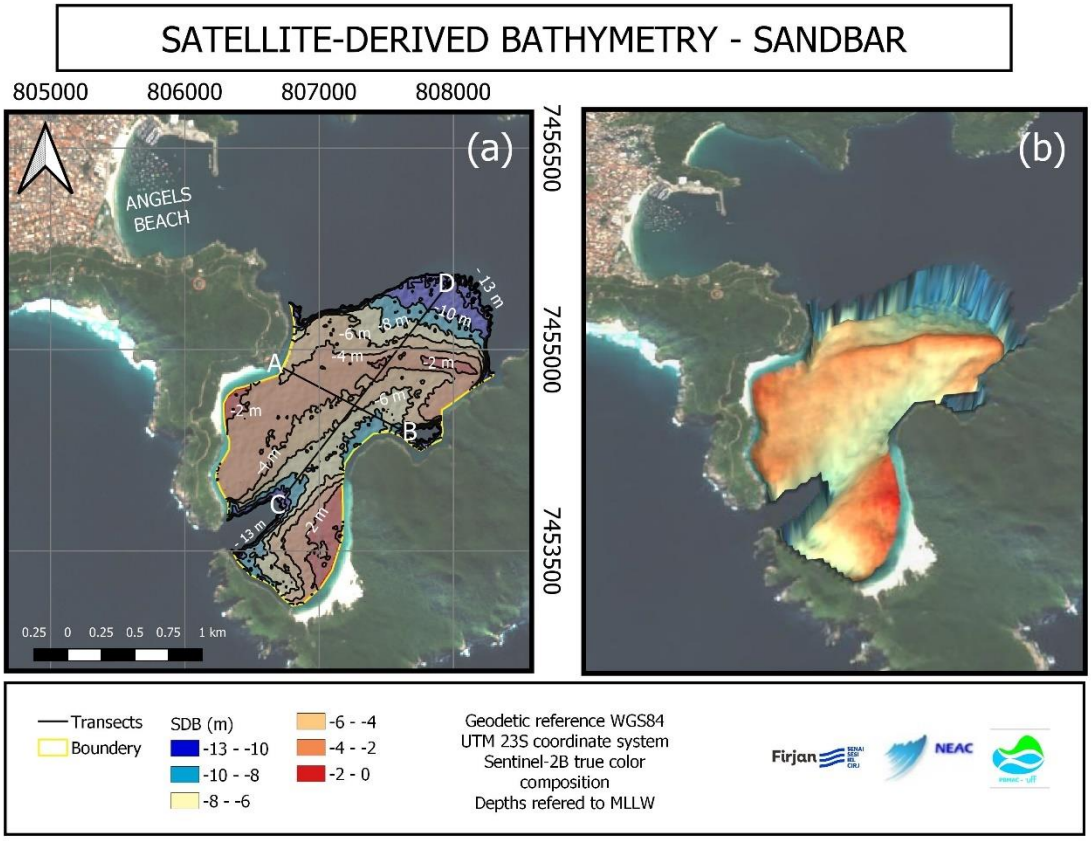

Figure 12. SDB of the submerged sandbar and longitudinal and cross-shore transects A and B for bathymetric profiles extraction on the left. A 3D perspective view of the sandbar on the right.

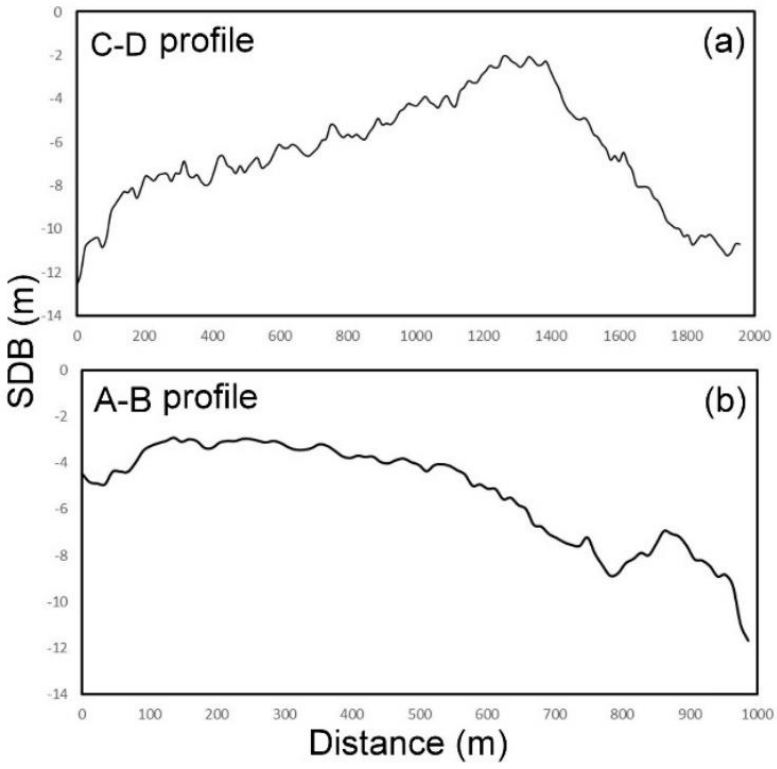

Figure 13. Bathymetric profiles extracted from the SDB of the submerged sandbar. (a) Longitudinal C-D profile. (b) Cross-shore A-B profile.

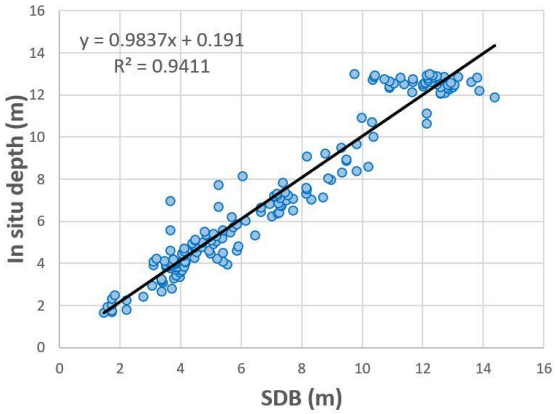

Figure 14. Scatter plot of the submerged sandbar SDB versus *in situ* depth points (n = 177).

Table 7. Statistical parameters of validation of the submerged sandbar SDB considering 0-13 m depth range.

Statistics	*r*	r^2	P-value for *r*	MAE (meters)	RMSE (meters)	n (check points)
SDB (Stumpf) x Depth points (Check)	0.97	0.94	P < 0.01	0.65	0.89	177

4. Discussion

All SDBs models of both applied methodologies on Anjos Beach resulted in similar geomorphological features (Figures 5 and 7) and statistical parameters. Also, all SDBs on Anjos Beach resulted in RMSE ≅ 1.0 m (Tables 2 and 4), with practically no difference between the models calibrated with 100% or 50% of the control points. Thus, the results found in this study corroborate with the previous results found by Vargas et al. (2021), in which the authors found a strong correlation between *in situ* data and satellite image.

Regarding coastal geomorphological dynamics, some authors have demonstrated the applicability of SDB for coastal geomorphological and sedimentary analyses. Misra and Ramakrishnan (2020) carried out a SDB monitoring to assess the impacts of a beach restoration program in India, extracting and comparing bathymetric profiles (transects) elaborated from satellite images and echo sounding data, and Alevizos, Roussos and Alexakis (2022) analyzed the evolution of nearshore bedforms by SDB on island of Crete, based on temporal mapping of crescentic sand bars.

In this study, the bathymetric maps on Anjos Beach (Figures 5, 7 and 10) illustrate the sedimentary conditions reported by Savi (2007), Motta et al. (2018) and Colaço et al. (2021), in which it is evidenced, mainly by the isobaths of -4 and -6 meters, their positions tending towards the inland continent (erosion) in the southern region of the beach and a sedimentation in the central part, represented by the spacing of these isobaths (-4 and -6 m). The cutfill map (Figure 10) represented an erosion region in front of the IEAPM and a region of deposition in the central and northern part of the beach, although there was also a deposition region to the south. The results corroborate with those verified by Colaço et al. (2021) in a short-term analysis, where the authors recorded a percentage of negative sedimentation in the southern region and a positive percentage in the central region in a period of 10 months.

Also, Savi (2007) identified distinct morphodynamic patterns on Anjos Beach from beach profiles analysis, noting that the beach can respond as totally reflective state, or reflective to the north and intermediate state to the south depending on the hydrodynamic conditions, with the northern region being characterized by low wave energy and, to the south, higher energy due to the interference caused by the breakwater in the waves arriving on

the beach. The aforementioned author also reports a sediment accumulation in the northern region of the beach, indicating a possible direction of the longshore drift from south to north. The bathymetric profiles extracted from the SDBs (Figure 9) show the same trend when compared with the depths by echo sounding. Although all profiles had an RMSE < 1 m, errors greater than 0.5 m are usually found in mappings from medium resolution satellite images (Landsat and Sentinel-2), as indicated by Alevizos, Roussos and Alexakis (2022).

However, although the bathymetric maps may indicate sedimentary and morphological conditions on Anjos Beach that corroborate with authors mentioned above, the time interval of approximately one year between the SDBs (2019-2020) is not enough to fully understand the morphodynamics of the beach. Thus, a monitoring considering a longer time interval and also oceanographic and meteorological seasonal variations (good and bad weathers) are necessary to confirm the morphodynamic patterns of the beach.

In addition to oceanographic variables (waves, currents and tide), another factor that could induce sediment mobilization on Anjos Beach is the boat wakes generated by small boats intense traffic (illustrated in Figure 2a), due to fishing, commercial and tourist activities. This phenomenon is discussed by some authors, such as Bilkovic et al. (2019) in Chesapeak Bay and Meyers et al. (2021) in Tampa Bay. Thus, this situation at Anjos Beach should be evaluated by specific studies.

Regarding the submerged sandbar, Silva (2009) analyzed the granulometry of the sandbar in the years 2006 and 2007 and found the predominance of fine sand fraction, as well as Fonseca (2012), obtaining phi values ranging from 2.13 to 2.6 (Wentworth scale). Comparatively, at Anjos Beach, the granulometry was analyzed by Motta et al. (2018) and the authors found a predominance of fine sand (central and northern region, close to the beach) and medium sand (southern region, indicating higher energy oscillations).

From the SDB of the sandbar (Figure 12), the estimated sediment volume up to the –13m isobath was approximately 13,964,312,266 m^3 and area of 2,509,800 m^2, obtained from the "volume calculation tool" plugin in QGIS 3.10 software. Castro (2018) monitored the sandbar from official nautical charts elaborated by Brazilian Navy from 1936 to 1991 and verified its growth in extension, average length, area and volume. The difference in area and volume in this period was 310,851 m^2 and 1,157,772 m^3. However, the author did not specify which depth (isobath) was considered for the calculation. Nevertheless, Castro (2018) found a continuous depositional process between 1936 and 1991, as well as Silva (2009).

It is important to highlight that, for the SDB mapping, 256 depth points were measured *in situ* only in a small region of the submerged sandbar and used for image calibration (Figure 3c). Even so, it was possible to estimate depths of distant areas up to -13 m covering its entire extension, where there are no *in situ* measured depth points.

As previously mentioned by Savi (2007), Motta et al. (2018) and Colaço et al. (2021), Anjos Beach undergoes erosion processes in its southern region and, one of the possible solutions to solve this problem, is beach nourishment, considered as a "soft engineering" (BIRD; LEWIS, 2015). The sediments that serve for beach nourishment should be as close as possible to the eroded beach in order to minimize transport costs, and a beach is more likely to be nourished if the sediment source area exists within an economically viable distance between them (BIRD; LEWIS, 2015). Among the different sources of sediments that may exist in different environments, those from port regions and sea floor can be considered, according to Bird and Lewis (2015).

The sandbar (Figure 12) can be a possible source of sediments for beach nourishment projects, since the location of the deposit near to the native beach and its granulometry and volume are essential characteristics that must be considered. According to Mangor et al. (2017), the success of a beach nourishment project depends on the grain size of the deposit in relation to the receiving native beach, as this will implicate on the morphodynamic conditions of the beach and coastal profile. Although the submerged sandbar can be a possible source of sediment for a beach nourishment project at Anjos Beach to minimize coastal erosion process, more specific studies of environmental impacts and coastal engineering must be carried out to determine the viability of the project, as well as other possible alternatives should be also evaluated. However, the same methodology that serves to map the submerged zone of the active profile of a sandy beach environment (SDB) also serves to map other coastal features, such as submerged sandbars.

On the other hand, the ports in coastal regions can directly benefit from SDB mapping for environmental monitoring and port management purposes, as the models offer a quick estimation of the submerged relief and sedimentary dynamics (MATEO-PÉREZ et al., 2020; MISRA; RAMAKRISHNAN, 2020; ALEVIZOS; ROUSSOS; ALEXAKIS, 2022). Some examples of SDB studies that were conducted in port regions are that by Mohamed et al.

(2017) in Egypt, Kimeli et al. (2018) in Kenya, Parente and Pepe (2018) in Portugal, Alves et al. (2018) in Brazil, Mateo-Pérez et al. (2020, 2021) in Spain, and Wu, Mao and Shen (2021) in China.

Mateo-Pérez et al. (2021) present a temporal series of dredging from SDBs in the Port of Luarca, where they could determine excavation and fill rates from the mapped bathymetries, with the aim of investigating whether the sedimentary dynamics is altered by dredging depth. The authors obtained values of $r^2 = 0.974$ and RMSE = 0.37 using Sentinel-2 images and echo sounding, suggesting the application in other ports. However, although there are several studies about SDBs, they may differ in terms of methodology (algorithms) and data used (satellite images, *in situ* depths, nautical charts etc.).

Also, it is evidenced that, even with a 50% reduction in the control points used for image calibration, the SDBs on Anjos Beach responded statistically similar to the models calibrated with 100% of the control points. This 50% reduction translates into lower cost and time of field surveys and data processing, as it means less need to survey depth points *in situ* by eco sounding. In addition, the amount and processing time of GNSS data will also be less.

Table 8. Costs and time estimations for bathymetric mapping on Anjos Beach by remote sensing considering 100% and 50% of the control points and a group of three professionals. $1 = BRL 5.24 (quote from Central Bank of Brazil, March 13th, 2023).

COSTS AND TIME	**100% of depth points measured *in situ* (n=313)**	**50% of depth points measured *in situ* (n=156)**
Field survey time estimation	6h	3h
Service cost per person (field survey considering 3 professionals)	$40/h (R$209.6 /h)	
Boat rental	$190.83 (R$ 1000)	$95.41 (R$ 500)
*Trip cost (for field survey)	$52,03 (R$272.64)	
QGIS software (license cost)	$0	
**ArcGIS software (license cost for personal use)	$100/yr (R$ 523.94/yr)	
Processing time (cost/hour – one professional)	6 days (8h/day) $40/h (R$ 209.6/h)	3 days (8h/day) $40/h (R$ 209.6/h)
***Daily cost (for 3 professionals)	$174.16 (R$ 912.6)	$87.08 (R$ 456.3)
TOTAL COST (not considering ArcGIS)	$3,057.02 (R$16,018.78)	$1,554.52 (R$8,145.68)

* Travel from Federal Fluminense University (UFF) in Niterói municipality, RJ, to Anjos Beach (300 km round trip) considering $27.82 of fuel, $5.21 of tolls and car rental of $19.
** ArcGIS license cost available on https://www.esri.com/pt-br/arcgis/products/arcgis-desktop/buy. This was not included in the calculations once there is the free QGIS software alternative.
*** Official daily price for field activities provided by UFF available on http://www.compras.uff.br/?q=content/di%C3%A1rias-e-passagens.

Table 8 provides time and cost estimations for SDB mapping, showing that costs can be reduced by approximately 50% when considering half of the control points. However, the values may vary depending on the number of people working and the displacement distance to the study area. Although the mapped area by echo sounder *in situ* was the same in all cases, the results obtained indicate that the navigated rout could be sparser (and not too dense), since the reduction of the calibration points for satellite image calibration did not interfere in the quality of the SDB models.

Although this reduction in calibration points of 50% was sufficient for bathymetric mapping, the results obtained are related to the specificities of the study area (costs, distance, logistics, etc.), as well as the number of depth points measured in the field. However, the methodology used (Figure 4) can be applied and evaluated in other regions of the Brazilian coast, considering the characteristics and peculiarities of each area. In addition, the absolute number of depth points measured *in situ* can also be evaluated for each case in order to obtain a reduction in the number of points that allow generating bathymetric model, statistically and geomorphologically.

On this point, for example, Santos Port (state of São Paulo) and the Organized Port of Rio Grande (Rio Grande Port - state of Rio Grande do Sul) have a series of PBAs of different themes related to port environmental management (KOEHLER; ASMUS, 2010; BRAZ; PIMENTEL; SILVA, 2015; SANTOS PORT AUTHORITY, 2022). Both ports have in their PBAs monitoring activities related of coastal sedimentary dynamics, such as topographic beach profile (Santos Port) and coastline (Rio Grande Port), in which bathymetry is an indispensable variable for the morphological analysis, and it is requested by public environmental authorities (SUPERINTENDÊNCIA DOS PORTOS DO RIO GRANDE DO SUL – SUPRG, 2020; SANTOS PORT AUTHORITY, 2022).

Alves et al. (2018) carried out a study in a coastal lagoon environment (Lagoa dos Patos, southern Brazil) where Rio Grande Port is located and concluded that the results obtained from the Landsat 8 images allowed mapping shapes and depth of the port access channel, serving as a low-cost tool. Krug and Noernberg (2007) estimated the bathymetry of Laranjeiras Bay located in an estuarine complex where Paranaguá Port is situated. The authors used Landsat 7 images and *in situ* data provided by Directorate of Hydrography and Navigation of the Brazilian Navy (DHN) and concluded that the methodology and results may be useful for geomorphological studies and environmental modeling.

For future works, the WPM sensor of the Chinese-Brazilian satellite CBERS-4A, lunched on December 20th, 2019 can be evaluated for SDB mapping, as it provides a pan chromatic band with spatial resolution of 2 m, which can be advantageous to reduce the errors. However, its low temporal resolution of 31 days can be an impediment.

5. Conclusion

Bathymetry is a crucial information for many applications, from habitat mapping to engineering projects. The monitoring of submerged reliefs in coastal environments such as sandy beaches and sandbars are practical cases of how bathymetry helps in the understanding of sedimentary dynamics.

Techniques and technologies for bathymetric mapping have evolved, mainly throughout the 20th century, in which depth information can currently be extracted from multispectral optical satellite images. SDB offers a low-cost alternative for quickly mapping the depth of a coastal environment and is a useful technique to complement a previously performed high detail bathymetric mapping, to perform higher frequency monitoring, and to serve as a preliminary study for bathymetric and geomorphological mappings that require a higher level of detail. Yet, this method is not recommended for navigation purposes, due to uncertainties and depth overestimation and underestimation.

This study demonstrated the possibility of mapping the bathymetry of two coastal environments, Anjos Beach and a submerged sandbar feature by remote sensing data and by two empirical methodologies, in which no significant differences were observed between them (statistically and geomorphologically). Also, the time and costs

estimation for bathymetric mapping of Anjos Beach demonstrated that, when considering half of the control points, the total cost for the mapping is estimated to reduce by approximately 50%.

Bathymetric mappings by remote sensing data in order to assist in the submerged geomorphology monitoring can be a low-cost alternative that could be incorporated into environmental management programs. Furthermore, this approach can be evaluated in different ports along the Brazilian coast but considering the water quality and local limitations. In addition, other themes for remote sensing mapping can be assessed to integrated into port environmental monitoring programs, such as chlorophyll-a concentration, sea surface temperature and oil spill detection.

Contribuições dos Autores: "Concepção, Ruan Vargas; metodologia, Ruan Vargas; software, Ruan Vargas, Camila Américo dos Santos; validação, Ruan Vargas; análise formal, Ruan Vargas; pesquisa, Ruan Vargas, Camila Américo dos Santos, Fábio Ferreira Dias e Julio Cesar de Faria Alvim Wasserman; recursos, Fábio Ferreira Dias e Julio Cesar de Faria Alvim Wasserman; preparação de dados, Ruan Vargas, Fábio Ferreira Dias, Julio Cesar de Faria Alvim Wasserman; escrita do artigo, Ruan Vargas e Fábio Ferreira Dias; revisão, Julio Cesar de Faria Alvim Wasserman, Camila Américo dos Santos, Agenor Cunha da Silva; supervisão, Fábio Ferreira Dias. Todos os autores leram e concordaram com a versão publicada do manuscrito".

Financiamento: Esta pesquisa foi financiada pela Coordenação de Aperfeiçoamento de Pessoal de Nível Superior – CAPES, por meio de bolsa de Pós-graduação (doutorado).

Agradecimentos: Agradecemos ao Núcleo de Estudos em Ambientes Costeiros (NEAC) da UFF e ao Programa de Pós-graduação de Biologia Marinha e Ambientes Costeiros da UFF.

Conflito de Interesse: Os autores declaram não haver conflito de interesse. Os financiadores não tiveram interferência no desenvolvimento do estudo; na coleta, análise ou interpretação dos dados; na redação do manuscrito, ou na decisão de publicar os resultados.

References

1. ALBERT, A.; MOBLEY, C. D. An analytical model for subsurface irradiance and remote sensing reflectance in deep and shallow case-2 waters. **Optics Express**, v. 11, n. 2, p. 2873-2890, 2003. DOI: 10.1364/OE.11.002873
2. ALEVIZOS, E.; ROUSSOS, A.; ALEXAKIS, D. D. Geomorphometric analysis of nearshore sedimentary bedforms from high-resolution multi-temporal satellite-derived bathymetry. **Geocarto International**, v. 37, n. 25, p. 8906-8923, 2022. DOI: 10.1080/10106049.2021.2007296
3. ALVES, D. C. L.; ESPINOZA, J. M. A.; ALBUQUERQUE, M. G.; SILVA, M. B.; FONTOURA, J. S.; SERPA, C.; WESCHENFELDER, J. Bathymetry estimation by orbital data of OLI sensor: A case study of the Rio Grande Harbor, southern Brazil. **Journal of Coastal Research**, SI (85), p. 51-55, 2018. DOI: 10.2112/SI85-011.1
4. ASHPHAQ, M.; SRIVASTAVA, P. K.; MITRA, D. Review of near-shore satellite derived bathymetry: Classification and account of five decades of coastal bathymetry research. **Journal of Ocean Engineering and Science**, v. 6, n. 4, p. 340-359, 2021. DOI: 10.1016/j.joes.2021.02.006
5. ATKINSON, A. L.; BALDOCK, T. E.; BIRRIEN, F.; CALLAGHAN, D. P.; NIELSEN, P.; BEUZEN, T.; TURNER, I. L.; BLENKINSOPP, C. E.; RANASINGHE, R. Laboratory investigation of the bruun rule and beach response to sea level rise. **Coasal Engineering**, v. 136, p. 183-202, 2018. DOI: 10.1016/j.coastaleng.2018.03.003
6. BARBOSA, D. S., ANJOS; A. P. A.; ALBUQUERQUE, A. L. S.; SIFEDDINE, A. Sedimentação orgânica na Lagoa Brejo do Espinho, Cabo Frio (RJ): Composição e implicações paleoclimáticas. In: Anais IX Congresso da Associação Brasileira de Estudos do Quaternário, 2003, Recife. **Anais...**
7. BILKOVIC, D. M.; MITCHELL, M. M.; DAVIS, J.; HERMAN, J.; ANDREWS, E.; KING, A.; MASON, P.; TAHVILDARI, N.; DAVIS, J.; DIXON, R. L. Defining boat wake impacts on shoreline stability toward management and policy solutions. **Ocean and Coastal Management**, v. 182, 2019.
8. BIRD, E. **Coastal geomorphology an introduction**. 2 Ed. England: John Wiley & Sons, 2008. 411 p.
9. BIRD, E.; LEWIS, N. **Beach renourishment**. Springer Cham, 2015.
10. BITAN, M.; ZVIELY, D. Sand beach nourishment: Experience from the Mediterranean Coast of Israel. **Journal of Marine Science and Engineering**, v. 8, 2020. DOI: 10.3390/jmse8040273
11. BRAZ, E. M. Q.; PIMENTEL, A. A.; SILVA, E. V. Gestão ambiental e os portos brasileiros: ênfase ao Porto de Santos - SP. **Revista Engenharia Ambiental - Espírito Santo do Pinhal,** v. 12, n. 1, p. 92-101, 2015.
12. BRUUN, P. Sea-level rise as a cause of shore erosion. **Journal of the waterways and harbors division**, v.88, p. 117-130, 1962. DOI: 10.1061/JWHEAU.0000252

13. BULHÕES, E.; FERNANDEZ, G. B.; OLIVEIRA FILHO, S. R.; PEREIRA, T. G.; ROCHA, T. B. Impactos costeiros induzidos por ondas de tempestade entre o Cabo Frio e o Cabo Búzios, Rio de Janeiro, Brasil. **Quaternary and Environmental Geosciences**, v. 5, n. 1, p. 154-165, 2014.
14. CABALLERO, I.; STUMPF, R. P. Retrieval of nearshore bathymetry from Sentinel-2A and 2B satellites in South Florida coastal waters. **Estuarine, Coastal and Shelf Sciences**, v. 226, 2019. DOI: 10.1016/j.ecss.2019.106277
15. CABALLERO, I.; STUMPF, R. P. Towards routine mapping of shallow bathymetry in environments with variable turbidity: Contribution of Sentinel-2A/B satellites mission. **Remote Sensing,** v. 12, p. 1-23, 2020. DOI: 10.3390/rs12030451
16. CAHALANE, C.; MAGEE, A.; MONTEYS, X.; CASAL, G.; HANAFIN, J.; HARRIS, P. A comparison of Landsat 8, RapidEye and Pleiades products for improving empirical predictions of satellite-derived bathymetry. **Remote Sensing of Environment**, v. 233, 2019. DOI: 10.1016/j.rse.2019.111414
17. CARVALHO, L. L.; DIAS, F. F.; SOUZA, V. S. M.; SILVA, A. L.; SANTOS, P. R. A.; VARGAS, R.; VILLAÇA, R. C. Solução de baixo custo para correção de variações de maré no mapeamento de ambientes costeiros. **Revista Brasileira de Geografia Física**, v. 11, n. 3, p. 904-912, 2018.
18. CASAL, G.; HARRIS, P.; MONTEYS, X.; HEDLEY, J.; CAHALANE, C.; MCCARTHY, T. Understanding satellite-derived bathymetry using Sentinel 2 imagery and spatial prediction models. **GIScience and Remote Sensing**, v. 57, p. 271-289, 2019. DOI: 10.1080/15481603.2019.1685198
19. CASTRO, J. V. A. The Morphodynamics Behaviour of a Cross-Shore Sandbar in a Microtidal Environment, Anjos Cove, Arraial do Cabo, Rio de Janeiro – Brazil. In: BOTERO, C.; CERVANTES, O.; FINKL, C. (Eds.). **Beach Management Tools - Concepts, Methodologies and Case Studies. Coastal Research Library.** Springer, 2018. DOI: 10.1007/978-3-319-58304-4_16
20. CHÉNIER, R., FAUCHERR, M-A., AHOLA, R. Satellite-derived bathymetry for improving canadian hydrographic service charts. **International Journal of Geo-Information**, v. 7, p. 1-15, 2018. DOI: 10.3390/ijgi7080306
21. COLAÇO, G.; VIOLANTE-CARVALHO, N.; ARRUDA, W. Z.; D`AVILA, V.; VILHENA, H.; FILIPPO, A.; CANDELLA, R. Mid-long term characterization and short term modelling of a semi-protected pocket sandy beach in the southern coast of Brazil. **Regional Studies in Marine Science**, v. 41, 2021. DOI: 10.1016/j.rsma.2020.101593
22. CONTI, L. A.; MOTA, G. T.; BARCELLOS, R. L. High-resolution optical remote sensing for coastal benthic habitat mapping: A case study of the Suape Estuarine-Bay, Pernambuco, Brazil. **Ocean and Coastal Management**, v. 193, 2020. DOI: 10.1016/j.ocecoaman.2020.105205
23. COOPER, J. A. G.; PILKEY, O. H. Sea-level rise and shoreline retreat: time to abandon the bruun rule. **Global and Planetary Change**, v. 43, p. 157-171, 2004. DOI: 10.1016/j.gloplacha.2004.07.001
24. COZANNET, G. L.; OLIVEROS, C.; CASTELLE, B.; GARCIN, M.; IDIER, D.; PEDREROS, R.; ROHMER, J. Uncertainties in sandy shorelines evolution under the bruun rule assumption. **Frontiers in Marine Science**, v. 3, n. 49, 2016. DOI: 10.3389/fmars.2016.00049
25. DIAS, L. F. L.; CASTRO, J. W. A.; SEOANE, J. C. S. Transição Pleistoceno-Holoceno na Enseada dos Anjos, Arraial do Cabo/Rio de Janeiro: Reconstrução paleoambiental 3D. **Revista Brasileira de Cartografia**, v. 66, n. 5, p. 931-951, 2014. DOI: 10.14393/rbcv66n5-44692
26. DIERSSEN, H. M.; THEBERGE, JR, A. E. 2014. Bathymetry: History of seafloor mapping. In: WANG, Y. (Ed.) **Encyclopedia of Natural Resources - Water and Air - Vol II**. Boca Raton: CRC Press, 2014, p. 644-648.
27. EL-HATTAB, A. I. Single beam bathymetric data modeling techniques for accurate maintenance dredging. **The Egyptian Journal of Remote Sensing and Space Sciences**, v. 17, n. 2, p. 189-195, 2014. DOI: 10.1016/j.ejrs.2014.05.003
28. EUROPEAN SPACE AGENCY - ESA. **Sentinel-2 User Handbook**. 2015. Disponível em: < https://sentinels.copernicus.eu/documents/247904/685211/Sentinel-2_User_Handbook.pdf/8869acdf-fd84-43ec-ae8c-3e80a436a16c?t=1438278087000>. Acesso em: 05 jun 2022
29. EVAGOROU, E.; METTAS, C.; AGAPIOU, A.; THEMISTOCLEOUS, K.; HADJIMITSIS, D. Bathymetric maps from multi-temporal analysis of Sentinel-2 data: the case study of Limassol, Cyprus. **Advances in Geosciences**, v. 45, p. 397-407, 2019. DOI: 10.5194/adgeo-45-397-2019
30. FERREIRA, C. E. L. **Partilha de recursos por herbívoros em um costão rochoso tropical, Arraial do Cabo, RJ**. Tese (Doutorado em Ecologia e Recursos Naturais) – Programa de Pós-Graduação em Ecologia e Recursos Naturais, Universidade Federal de São Carlos, São Paulo. 1998. 87 p.
31. FIGUEIREDO JR, A. G., PACHECO, C. E. P., VASCONCELOS, S. D., SILVA, F. T. Geomorfologia e sedimentologia da plataforma continental. In: Kowsmann, R. O. (Ed.). **Geologia e geomorfologia**. Rio de Janeiro: Elsevier, 2015, p. 13-32.

32. FILHO, S. R. O.; SANTOS, R. A.; FERNANDEZ, G. B. Erosão e recuperação de praias refletivas de alta energia impactadas por ondas de tempestade geradas por ciclone tropical. **Revista Brasileira de Geomorfologia**, v. 21, n. 2, p. 289-312, 2020. DOI: 10.20502/rbg.v21i2.1455
33. FONSECA, R. B. M. Evolução batimétrica e sedimentológica do banco de areia "*sandbar*" da Enseada dos Anjos, Arraial do Cabo – Rio de Janeiro. Dissertação (Mestrado em Geologia) – Programa de Pós-Graduação em Geologia, Universidade Federal do Rio de Janeiro, Rio de Janeiro. 2012. 106p.
34. FOX-KEMPER, B., HEWITT, H. T.; XIAO, C.; AÐALGEIRSDÓTTIR, G.; DRIJFHOUT, S. S.; EDWARDS, T. L.; GOLLEDGE, N. R.; HEMER, M.; KOPP, R. E.; KRINNER, G.; MIX, A.; NOTZ, D.; NOWICKI, S.; NURHATI, I. S.; RUIZ, L.; SALLÉE, J.-B.; SLANGEN, A. B. A.;YU, Y. Ocean, Cryosphere and Sea Level Change. In: MASSON-DELMOTTE, V., ZHAI, P.; PIRANI, A.; CONNORS, S. L.; PÉAN, C.; BERGER, S.; CAUD, N.; CHEN, Y.; GOLDFARB, L.; GOMIS, M. I.; HUANG, M.; LEITZELL, K.; LONNOY, E.; MATTHEWS, J. B. R.; MAYCOCK, T. K.; WATERFIELD, T.; YELEKÇI, O.; YU, R.; ZHOU, B. (Eds.). **Climate Change 2021: The Physical Science Basis**. United Kingdom and New York: Cambridge University Press, 2021. p. 1211–1362.
35. GABR, B.; AHMED, M.; MARMOUSH, Y. PlanetScope and Landsat 8 imageries for bathymetry mapping. **Journal of Marine Science and Engineering**, v. 8, n. 2, 2020. DOI: 10.3390/jmse8020143
36. GAO, J. Bathymetry mapping by means of remote sensing: methods, accuracy and limitations. **Progress in Physical Geography**, v. 33, p. 103-116, 2009. DOI: 10.1177/0309133309105657
37. GREEN, E., EDWARDS, A., MUMBY, P. Mapping bathymetry. In: EDWARDS, A. J. (Ed.) **Remote sensing handbook for tropical coastal management.** Paris: UNESCO publishing, 2000. p. 219-233.
38. HEDLEY, J. D.; HARBORNE, A. R.; MUMBY, P. J. Technical note: Simple and robust removal of sun glint for mapping shallow-water benthos. **International Journal of Remote Sensing**, v. 26, p. 2107–2112, 2005. DOI: 10.1080/01431160500034086
39. JESUS, P. B., DIAS, F. F.; MUNIZ, R. A.; MACÁRIO, K. C. D.; SEOANE, J. C. S.; QUATTROCIOCCHI, D. G. S.; CASSAB, R. C. T.; AGUILERA, O.; SOUZA, R. C. C. L.; ALVES, E. Q.; CHANCA, I. S.; CARVALHO, C. R. A.; ARAÚJO, J. C. Holocene paleo-sea level in southeastern Brazil: an approach based on vermetids shells. **Journal of Sedimentary Environments**, v. 2, n. 1, 2017. DOI: 10.12957/jse.2017.28158
40. KIM, H.; LEE, S. B.; MIN, K. S. Shoreline change analysis using airborne LiDAR bathymetry for coastal monitoring. **Journal of Coastal Research**, SI(79), p. 269-273, 2017. DOI: 10.2112/SI79-055.1
41. KIMELI, A.; THOYA, P.; NGISIANG`E, N.; ONG`ANDA, H.; MAGORI, M. Satellite-derived bathymetry: a case study of Mombasa Port Channel and its approaches, Kenya. **WIO Journal of Marine Science**, v. 17, p. 93-102, 2018. DOI: 10.4314/wiojms.v17i2.8
42. KITZMANN, D. I. S.; ASMUS, M. L.; KOEHLER, P. H. W. Gestão ambiental portuária: desafios, possibilidades e inovações em um contexto de globalização. **Espaço Aberto**, v**.** 5, n. 2, p. 147-164, 2014. DOI: 10.36403/espacoaberto.2014.3308
43. KOEHLER, P. H. W.; ASMUS, M. L. Gestão integrada em Portos Organizados: uma análise baseada no caso do porto de Rio Grande, RS-Brasil. Revista da Gestão Costeira Integrada, v. 10, n. 2, p. 201-215, 2010.
44. KRUG, L. A.; NOERNBERG, M. A. O sensoriamento remoto como ferramenta para determinação de batimetria de baixios na Baía das Laranjeiras, Paranaguá-PR. **Revista Brasileira de Geofísica**, v. 25(supl.1), p. 101-105, 2007. DOI: 10.1590/S0102-261X2007000500010
45. KUDALE, M. D. Impact of port development on the coastline and the need for protection. **Indian Journal of Geo-Marine Science**, v. 39, n. 4, p. 597-604, 2010.
46. KUMARI, P.; RAMESH, H. Remote sensing image based nearshore bathymetry extraction of Mangaluru coast for planning coastal reservoir. In: SITHARAM, T. G.; YANG, S-Q.; FALCONER, R.; SIVAKUMAR, M.; JONES, B.;
47. LEATHERMAN, S. P., DOUGLAS, B. C., LABRECQUE, J. L. Sea level and coastal erosion require large-scale monitoring. **Eos**, v. 84, 2003. DOI: 10.1029/2003EO020001
48. LEATHERMAN, S. P., ZHANG, K., DOUGLAS, B. C. Sea level rise shown to drive coastal erosion. **Eos**, v. 81, 2000. DOI: 10.1029/00EO00034
49. LEDER, T. D.; BAUCIC, M.; LEDER, N.; GILIC, F. Optical Satellite-Derived Bathymetry: An Overview and WoS and Scopus Bibliometric Analysis. **Remote Sensing**, v. 15, 2023. DOI: 10.3390/rs15051294
50. LIMA, F. A. V. Portos marítimos e os desafios para a sustentabilidade costeira. In: SOUTO, R. D. (Org.). **Gestão Ambiental e Sustentabilidade em Áreas Costeiras e Marítimas: Conceitos e Práticas**. Rio de Janeiro: Instituto Virtual para o Desenvolvimento Sustentável - IVIDES.org, 2020. p.198-229.

51. LUDKA, B. C.; GUZA, R. T.; O´REILLY, W. C.; MERRIFIELD, M. A.; FLICK, R. E.; BAK, A. S.; HESSER, T.; BUCCIARELLI, R.; OLFE, C.; WOODWARD, B.; BOYD, W.; SMITH, K.; OKIHIRO, M.; GRENZEBACK, R.; PARRY, L.; BOYD, G. Sixteen years of bathymetry and waves at San Diego beaches. **Scientific Data,** v. 6, n. 161, 2019. DOI: 10.1038/s41597-019-0167-6
52. LUIJENDIJK, A., HAGENAARS, G., RANASINGHE, R., BAART, F., DONCHYTS, G., AARNINKHOF, S. The state of the world´s beaches. **Scientific Reports**, v. 8, 2018. DOI: 10.1038/s41598-018-24630-6
53. LYZENGA, D. R. Passive remote sensing techniques for mapping water depth and bottom features. **Applied Optics**, v. 17, p. 379-383, 1978. DOI: 10.1364/AO.17.000379
54. LYZENGA, D. R. Shallow-water Bathymetry using combined LiDAR and Passive Multispectral Scanner Data. **International Journal of Remote Sensing**, v. 6, p. 115–125, 1985. DOI: 10.1080/01431168508948428
55. MANGOR, K.; DRØNEN, N. K.; KÆRGAARD, K. H.; KRISTENSEN, S. E. **Shoreline management guidelines**. Dinamarca: DHI, 2017. 461p.
56. MATEO-PÉREZ, V.; CORRAL-BOBADILLA, M.; ORTEGA-FERNÁNDEZ, F.; RODRÍGUEZ-MONTEQUÍN, V. Analysis of the spatio-temporal evolution of dredging from satellite images: A case study in the Principality of Asturias (Spain). **Journal of Marine Sciences and Engineering**, v. 9, n. 267, 2021. DOI: 10.3390/jmse9030267
57. MATEO-PÉREZ, V.; CORRAL-BOBADILLA, M.; ORTEGA-FERNÁNDEZ, F.; VERGARA-GONZÁLEZ, E. P. Port bathymetry mapping using support vector machine technique and Sentinel-2 satellite imagery. **Remote Sensing**, v. 12, 2020. DOI: 10.3390/rs12132069
58. MATSUBA, Y.; SATO, S. Nearshore bathymetry estimation by UAV. **Coastal Engineering Journal**, v. 60, n. 1, p. 51-59, 2018. DOI: 10.1080/21664250.2018.1436239
59. MCFEETERS, S. K. The use of normalized difference water index (NDWI) in the delineation of open water features. **International Journal of Remote Sensing**, v. 17, p. 1425-1432, 1996. DOI: 10.1080/01431169608948714
60. MELO, L. V.; SALES, T. B.; SOUZA, G. L.; BRANT, F. F.; MANICACCI, M. Ampliação do Porto do Forno na Reserva Extrativista Marinha em Arraial do Cabo-RJ. **Boletim do Observatório Ambiental Alberto Ribeiro Lamego**, v. 3, n. 2, p. 163-186, 2009.
61. MENANDRO, P. S.; BASTOS, A. C. Seabed mapping: A brief history from meaningful words**. Geosciences**, v. 10, p. 1-17, 2020. DOI: 10.3390/geosciences10070273
62. MEYERS, S. D.; LUTHER, M. E.; RINGUET, S.; RAULERSON, G.; SHERWOOD, E.; CONRAD, K.; BASILI, G. Ship wakes and their potential shoreline impact in Tampa Bay. Ocean & Coastal Management, v. 211, 2021. DOI: 10.1016/j.ocecoaman.2021.105749
63. MISRA, A.; RAMAKRISHNAN, B. Assessment of coastal geomorphological changes using multi-temporal Satellite-Derived Bathymetry. **Continental Shelf Research**, v. 207, 2020. DOI: 10.1016/j.csr.2020.104213
64. MOHAMED, H.; NEGM, A.; SALAH, M.; NADAOKA, K.; ZAHRAN, M. Assessment of proposed approaches for bathymetry calculations using multispectral satellite images in shallow coastal/lake areas: a comparison of five models. **Arabian Journal of Geoscience**, v. 10, n. 2, 2017. DOI: 10.1007/s12517-016-2803-1
65. MOTTA, P. R.; NETTO, L. R.; BASTOS, E. B.; PEREIRA, T. G.; BULHÕES E. M. R. Distribuição e transporte de sedimentos costeiros: exemplos em Arraial do Cabo, RJ. **Revista Brasileira de Geomorfologia**, v. 19, n. 2, p. 341-358, 2018. DOI: 10.20502/rbg.v19i2.1277
66. MOURA, R. F. **Do outro lado das pontes: História, etnografia e planejamento urbano numa cidade média do interior fluminense**. Dissertação (Mestrado em Antropologia) – Programa de Pós-Graduação em Antropologia, Universidade Federal Fluminense, Niterói. 2012.
67. MUEHE, D. (Org.). **Panorama da erosão costeira no Brasil**. Brasília: MMA, 2018. 759 p.
68. MUEHE, D. O litoral brasileiro e sua compartimentação. In: GUERRA, A. J. T.; CUNHA, S. B. (Org.). **Geomorfologia do Brasil.** Rio de Janeiro: Bertrand Brasil, 1998, p. 273-349.
69. MUEHE, D.; LINS-DE-BARROS, F. M. The beaches of Rio de Janeiro. In: SHORT, A. D.; KLEIN, A. H. F. (Eds.). **Brazilian beach systems**, Springer, 2016. p. 363-396.
70. NATIONAL AERONAUTICS AND SPACE ADMINISTRATION – NASA. **The science of sunglint**. 2021. Disponível: < https://earthobservatory.nasa.gov/images/84333/the-science-of-sunglint > Acesso em: 14 fev 2022.
71. NOUJAS, V.; THOMAS, K. V.; NAIR, L. S.; HAMEED, T. S. S.; BADAREES, K. O.; AJEESH, N. R. Management of shoreline morphological changes consequent to breakwater construction. **Indian Journal of Geo-Marine Sciences**, v. 43, n. 1, p. 54-61, 2014.
72. PARENTE, C.; PEPE M. Bathymetry from Worldview-3 satellite data using radiometric band ratio. **Acta Polytechnica**, v. 58, n. 2, p. 109-117, 2018. DOI: 10.14311/AP.2018.58.0109

73. PEREIRA, W. L. C. M. Vagas da modernidade: a Companhia Nacional de Álcalis em Arraial do Cabo (1943-964). **Estudos Históricos**, v. 23, n. 46, p. 321-343, 2010. DOI: 10.1590/S0103-21862010000200006
74. POLCYN, F. C., ROLLIN, R. A. Remote sensing techniques for the location and measurement of shallow-water features. Willow Run Laboratories, The University of Michigan, 1969.
75. PUIG, M.; WOOLDRIDGE, C.; MICHAIL, A.; DARBRA, R. M. Current status and trends of the environmental performance in European ports. **Environmental Science & Policy**, v. 48, p. 57-66, 2015. DOI: 10.1016/j.envsci.2014.12.004
76. QUADROS, P.; CASTRO, J. W. A.; GUEDES, E.; PEREIRA, V. C. R. Distribuição sazonal dos sedimentos na praia do Farol, Ilha do Cabo Frio, Arraial do Cabo, Rio de Janeiro. **Revista Brasileira de Geomorfologia, v.** 17, n. 2, 2016. DOI: 10.20502/rbg.v17i2.722
77. RATNAYAKE, N. P.; RATNAYAKE, A. S.; KEEGLE, P. V.; ARACHCHI, M. A. K. M. M.; PREMASIRI, H. M. R. An analysis of beach profile changes subsequent to the Colombo Harbor Expansion Project, Sri Lanka. **Environmental Earth Sciences**, v. 77, 2018. DOI: 10.1007/s12665-018-7234-8
78. REBOITA, M. S.; AMBRIZZI, T.; SILVA, B. A.; PINHEIRO, R. F.; ROCHA, R. P. The South Atlantic Subtropical Anticyclone: Present and future climate. **Frontiers in Earth Sciences**, v. 7, 2019. DOI: 10.3389/feart.2019.00008
79. ROSSI, L.; MAMMI I.; PELLICCIA, F. UAV-derived multispectral bathymetry. **Remote Sensing**, v. 12, 2020. DOI: 10.3390/rs12233897
80. SAENGSUPAVANICH, C.; SEENPRACHAWONG, U.; GALLARDO, W. G.; SHIVAKOTI, G. P. Port-induced erosion prediction and valuation of a local recreational beach. **Ecological Economics**, v. 67, p. 93-103, 2008. DOI: 10.1016/j.ecolecon.2007.11.018
81. SANTOS PORT AUTHORITY. 2022. **Estudos e Programas**. Disponível em: < https://www.portodesantos.com.br/comunidade-sustentabilidade/sustentabilidade/estudos-prgramas/> Acesso em: 17 ago 2022.
82. SAVI, D. C. 500 anos de ocupação portuguesa. Evolução histórica da Enseada dos Anjos, Arraial do Cabo, Rio de Janeiro, Brasil. In: Anais IX Congresso da Associação Brasileira de Estudos do Quaternário, 2003b, Recife. **Anais...**
83. SAVI, D. C. **Efeito da construção de um quebra mar sobre os processos morfodinâmicos e sedimentares na Enseada dos Anjos, Arraial do Cabo, RJ**. Dissertação (Mestrado em Geografia) – Programa de Pós-Graduação em Geografia, Universidade Federal do Rio de Janeiro, Rio de Janeiro. 2003a. 120p.
84. SAVI, D. C. Erosão e acresção costeira na Enseada dos Anjos, Arraial do Cabo, RJ. **Revista Brasileira de Geofísica**, v. 25, p. 91-99, 2007. DOI: 10.1590/S0102-261X2007000500009
85. SAVI, D. C.; FERNANDEZ, G. Efeitos da construção de um quebra-mar sobre a linha de costa e a batimetria da Enseada dos Anjos, Arraial do Cabo, Rio de Janeiro, Brasil. In: Anais IX Congresso da Associação Brasileira de Estudos do Quaternário, 2003, Recife. **Anais...**
86. SAYLAM, K.; HUPP, J. R.; AVERETT, A. R.; GUTELIUS, W. F.; GELHAR, B. W. Airborne lidar bathymetry: assessing quality assurance and quality control methods with Leica Chiroptera examples. **International Journal of Remote Sensing**, v. 39, n. 8, p. 2518-2542, 2018. DOI: 10.1080/01431161.2018.1430916
87. SILVA, A. C. **Dinâmica batimétrica e sedimentológica da região de Cabo Frio – estado do Rio de Janeiro**. Tese (Doutorado em Geologia) – Programa de Pós-Graduação em Geologia, Universidade Federal do Rio de Janeiro, Rio de Janeiro. 2009. 157p.
88. SOUZA, C. R. G., FILHO, P. W. M. S., ESTEVES, L. S., VITAL, H., DILLENBURG, S. R., PATCHINEELAM, S. M., ADDAD, J. E. **Praias arenosas e erosão costeira.** In: SOUZA, C. R. G., SUGUIO, K., OLIVEIRA, M. A. S., OLIVEIRA, P.E. (Eds.). Quaternário do Brasil. Ribeirão Preto: Holos Editora, 2005. p. 130-152.
89. STUMPF, R. P.; HOLDERIED, K.; SINCLAIR, M. Determination of water depth with high- resolution satellite imagery over variable bottom types. **Limnology and Oceanography**, v. 48, p. 547-556, 2003. DOI: 10.4319/lo.2003.48.1_part_2.0547
90. SUPERINTENDÊNCIA DOS PORTOS DO RIO GRANDE DO SUL – SUPRG. **Plano Básico Ambiental - PBA do Porto do Rio Grande**. 2020. Disponível em: < https://www.portosrs.com.br/site/public/uploads/site/resp-ambiental/71.pdf> Acesso em: 5 ago 2022.
91. VARGAS, R.; DIAS, F. F.; WASSERMAN, J. C. F. A.; SANTOS, P. R. A.; SILVA, A. L.; SANTOS, C. A.; FERREIRA, V. L. D.; BARCELOS, J. S. Mapeamento topobatimétrico do canal de maré da Lagoa de Araruama, Rio de Janeiro, Brasil. In: PAULA, D. P.; DIAS, J. A.; FONSECA, L. C.; RODRIGUES, M. A. C.; ALBUQUERQUE, M. G.; PALMA, M.; PEREIRA, S. D. (Eds.). **Diálogos em torno da linha de costa: O oceano que nos une.** Rio de Janeiro: FGEL-UERJ, 2020, p.53-62.
92. VARGAS, R.; WASSERMAN, J. C. F. A.; SILVA, A. L.; TAVARES, T. L.; SANTOS, C. A.; DIAS, F. F. Satellite-derived bathymetry models from Sentinel-2A and 2B in the coastal clear waters of Arraial do Cabo, Rio de Janeiro, Brazil. **Revista Brasileira de Geografia Física**, v. 14, n. 5, p. 3078-3095, 2021. DOI: 10.26848/rbgf.v14.5.p3078-3095

93. VILLENA, H. H.; CARVALHO, N. V.; FILIPPO, A. M.; D`ÁVILA, V. A.; PEREIRA, S. D.; DIAS, M. S.; CANDELLA, R. N.; PASSOS, G. C. M.; VIEIRA, Y. S. S. Morfologia de fundo e poluição por macrodetritos na Enseada dos Anjos, Arraial do Cabo-RJ. In: PEREIRA S. D.; RODRIGUES, M. A.; BERGAMASCHI, S.; FREITAS, J. G. (Eds.). **O Homem e as Zonas Costeiras**. Rio de Janeiro: FAPERJ, 2015. p. 74-88.
94. VOUSDOUKAS, M. I., RANASINGHE, R., MENTASCHI, L., PLOMARITIS, T. A., ATHANASIOU, P., LUIJENDIJK, A., FEYEN, L. Sandy coastlines under threat of erosion. **Nature Climate Change**, v. 10, 2020. DOI: 10.1038/s41558-020-0697-0
95. WESTLEY, K. Satellite-derived bathymetry for maritime archaeology: Testing its effectiveness at two ancient harbours in the Eastern Mediterranean. **Journal of Archeological Science: Reports**, v. 38, 2021. DOI: 10.1016/j.jasrep.2021.103030
96. WINCKLER, P.; MARTÍN, R. A.; ESPARZA, C.; MELO, O.; SACTIC, M. I.; MARTÍNEZ, C. Projections of beach erosion and associated costs in Chile. **Sustainability**, v. 15, 2023. DOI: 10.3390/su15075883
97. WU, Z.; MAO, Z.; SHEN, W. Integrating multiple datasets and machine learning algorithms for satellite-based bathymetry in seaports. **Remote Sensing**, **v.** 13, 2021. DOI: 10.3390/rs13214328
98. ZHANG, K., DOUGLAS, B. C., LEATHERMAN, S. P. Global warming and coastal erosion. **Climate change**, v. 64, 2004. DOI: 10.1023/B:CLIM.0000024690.32682.48